

A CRANIOMETRIC ANALYSIS OF DOGS (CANIS FAMILIARIS) FOR THE PURPOSE OF IDENTIFYING ARCHEOZOOLOGICAL MATERIAL

Kaloyianni, Olivia Frances

Master's thesis / Diplomski rad

2022

Degree Grantor / Ustanova koja je dodijelila akademski / stručni stupanj: **University of Zagreb, Faculty of Veterinary Medicine / Sveučilište u Zagrebu, Veterinarski fakultet**

Permanent link / Trajna poveznica: <https://um.nsk.hr/um:nbn:hr:178:586768>

Rights / Prava: [In copyright](#)/[Zaštićeno autorskim pravom.](#)

Download date / Datum preuzimanja: **2024-07-24**



Repository / Repozitorij:

[Repository of Faculty of Veterinary Medicine -
Repository of PHD, master's thesis](#)



UNIVERSITY OF ZAGREB
FACULTY OF VETERINARY MEDICINE

Olivia Frances Kaloyianni

**A CRANIOMETRIC ANALYSIS OF DOGS
(CANIS FAMILIARIS) FOR THE PURPOSE
OF IDENTIFYING
ARCHEOZOOLOGICAL MATERIAL**

Diploma thesis

Zagreb, 2022.

University of Zagreb

Faculty of Veterinary Medicine

Department of Anatomy, Histology and Embryology

Head of Department: Prof. Martina Đuras

Mentor: Prof. Tajana Trbojević Vukičević

Members of the Committee for the defence of Diploma thesis:

1. Prof. Martina Đuras
2. Associate prof. Ivan Alić
3. Prof. Tajana Trbojević Vukičević
4. Prof. Srebrenka Nejedli (substitute)

ACKNOWLEDGMENTS

I would like to thank Professor Tajana Trbojević Vukičević for her contributions to this study, for the opportunity to work with her in the field of archaeozoology and for her continuous support.

I would also like to thank Georgios Kalogiannis and Camilla Kate Barker for their contributions and advice throughout this study.

Lastly, I would like to thank Professor Martina Đuras and the Department of Anatomy, Histology and Embryology for providing me with this opportunity.

TABLE LIST

Table 1. Dog breeds and respective sample size

Table 2. Measurements used in the study by VON DEN DRIESCH (1976) and their corresponding name and description.

Table 3. Landmark definitions for dorsal aspect.

Table 4. Landmark definitions for ventral aspect.

Table 5. Landmark definitions for lateral aspect.

Table 6. Indices in their calculation formulas.

Table 7. Individual dog skull measurements and their respective breeds.

Table 8. Measurements made from digital images for the purpose of index calculations.

Table 9. Indices calculated from digital image-based measurements.

Table 10. Digital image-based measurements of representative skulls.

Table 11. Results from tests of normality in distribution. Statistic indicating test statistic, df as degrees of freedom. Asterisks indicating level of significance and NS nonsignificance.

FIGURE LIST

Figure 1. Dorsal aspect of dog skull with measurements by VON DEN DRIESCH (1976). The used measurements are marked in red.

Figure 2. Lateral aspect of dog skull with measurements by VON DEN DRIESCH (1976). The used measurements are marked in red.

Figure 3. Ventral aspect of dog skull with measurements by VON DEN DRIESCH (1976). The used measurements are marked in red.

Figure 4. Dorsal aspect landmarks on Skull 3.

Figure 5. Ventral aspect landmarks on Skull 3

Figure 6. Lateral aspect landmarks on Skull 3.

Figure 7. One-way ANOVA test results from the comparison of the measurements for M1 (Total length of skull) to each dog breed in the sample.

Figure 8. One-way ANOVA test results from the comparison of the measurements for M7 (Breadth of Foramen magnum) to each dog breed in the sample.

Figure 9. One-way ANOVA test results from the comparison of the measurements for M8 (Greatest breadth of braincase) to each dog breed in the sample.

Figure 10. One-way ANOVA test results from the comparison of the measurements for M9 (Zygomatic breadth). to each dog breed in the sample.

Figure 11. One-way ANOVA test results from the comparison of the measurements for M11 (Least palatal breadth (measure behind canines)) to each dog breed in the sample.

Figure 12. One-way ANOVA test results from the comparison of the measurements for M12 (Breadth at the canine alveoli) to each dog breed in the sample.

Figure 13. One-way ANOVA test results from the comparison of the measurements for M13 (Skull height) to each dog breed in the sample.

Figure 14. One-way ANOVA test results from the comparison of the measurements for M14 (Skull height without sagittal crest) to each dog breed in the sample.

Figure 15. Example of a Procrustes superimposition. Procrustes analysis of the ventral aspect landmarks of each dog skull in the sample.

Figure 16. Graphical representation of the results from comparing Principle Component 1 to Principle Component 2 of the dorsal aspect landmarks.

Figure 17. Wireframe comparison of dorsal landmarks from the Border terrier dog breed (dark blue) and the mean dorsal landmarks (light blue).

Figure 18. Wireframe comparison of dorsal landmarks from the Doberman dog breed (dark blue) and the mean dorsal landmarks (light blue).

Figure 19. Wireframe comparison of dorsal landmarks from the Dalmatian dog breed (dark blue) and the mean dorsal landmarks (light blue).

Figure 20. Graphical representation of the results from comparing Principle Component 1 vs Principle Component 2 of the lateral aspect landmarks.

Figure 21. Wireframe comparison of lateral landmarks from the Border terrier dog breed (dark blue) and the mean lateral landmarks (light blue).

Figure 22. Wireframe comparison of lateral landmarks from the Doberman dog breed (dark blue) and the mean lateral landmarks (light blue).

Figure 23. Wireframe comparison of lateral landmarks from the Newfoundland dog breed (dark blue) and the mean lateral landmarks (light blue).

Figure 24. Graphical representation of the results from comparing Principle Component 1 vs Principle Component 2 of the ventral aspect landmarks.

Figure 25. Wireframe comparison of ventral landmarks from the Border terrier dog breed (dark blue) and the mean landmarks (light blue).

Figure 26. Wireframe comparison of ventral landmarks from the Boxer dog breed (dark blue) and the mean landmarks (light blue).

Figure 27. Wireframe comparison of ventral landmarks from the Dalmatian dog breed (dark blue) and the mean ventral landmarks (light blue).

CONTENT

1. Introduction	1
2. Literature review	3
3. Materials and methods	5
4. Results	15
5. Discussion	36
6. Conclusions	40
7. Literature	41
8. Summary	44
9. Sažetak	45
10. Biography	46

1. INTRODUCTION

Craniometry is the study of measurements made from the structures of the skull and face in order to analyse the osseous features of different groups, such as those characterised by the same species, ethnicity, age category, or sex. These measurements are usually taken from craniometric points which are used as landmarks. Craniometry has been used in multiple disciplines, including anthropology, forensic science, archaeozoology, and neuroscience (VIGO et al., 2020).

VON DEN DRIESCH (1976) published a set of standard bone measurements for mammals and birds, which are the most widely used by analysts in various scientific fields. These measurements contribute to what is described as traditional morphometrics (MARCUS, 1990; REYMENT, 1991) or multivariate morphometrics (REYMENT, 1971), which are characterised by the application of multivariate statistical methods to a set of morphological variables.

In traditional morphometrics, one-dimensional measurements are used from two set points, usually describing distance, such as length, width, or height, but also ratios and angles can be added. They do not describe the set points in relation to other points on the specimen and often exhibit autocorrelation, isometry, and non-normal distribution (DRAKE et al., 2017). Furthermore, multivariate statistical methods cannot consider whether multiple measurements were made from a common landmark or if certain landmarks form a specific shape on the specimen. It is not possible to recover the shape of the original form from the usual data matrices of distance measurements (ROHLF and MARCUS, 1993).

In the case of geometric morphometrics, specifically landmark methods, two-dimensional (2D) or three-dimensional (3D) coordinates of morphological landmarks on the specimen are recorded in order to describe the shape of the specimen. These landmarks can be classified as either true, semi, or pseudo-landmarks. (BARDUA et al., 2019). The landmark coordinates cannot be directly analysed as variables until any non-shape variation is removed i.e., eliminating information pertaining to size, position, and rotation. By using a Generalised Procrustes Analysis, non-shape variations can be mathematically removed by superimposing landmark configurations based on an optimisation criterion, most commonly the least-squares estimates for translation and rotation parameters, whereas for size, by scaling all landmark configurations to the same centroid size (ADAMS et al., 2004).

In the field of archaeozoology, bone measurements are routinely taken and can contribute to researching the topics of domestication, herd management, hunting strategies and environmental changes (REITZ and WING, 1999). The possibility of being able to accurately identify or at least, narrow down the potential breed of an unknown dog skull found in archaeological excavations can provide us with knowledge about the type of breeds and their proximity to humans, their evolutionary changes from the past until the present day, their role in that society, their adaptations to the environment, and perhaps even shed light on certain pathological processes.

The purpose of this study is to conduct a craniometric analysis of domesticated dog skulls using the traditional morphometrics and geometric morphometrics to assess whether they can accurately identify the dog breed of each skull in the sample, as well as compare the results obtained from both methods.

2. LITERATURE REVIEW

ADAMS et al. (2004) published an article reviewing the advances made in morphometric studies during the previous decade. Here, they describe traditional and geometric morphometrics (outline and landmark methods) and speculate on the future of morphometrics. For traditional morphometrics, they raise the issue of correlation between size and linear measurements, the lack of agreement on a method for correcting size and that the same sets of linear distances can be taken by objects that have significantly different shapes. They conclude that it wasn't possible to use linear measurements to generate graphical representations of shape. In the case of geometric morphometrics, they present the progression and maturation of these methods, as well as the increase in popularity of these methods over the previous decade. They conclude that for most applications of landmark geometric morphometrics there are widely accepted standard protocols of Procrustes methods with added "extensions" for certain types of data. Furthermore, outline geometrics morphometrics can also be analysed using Procrustes methods through the use of sliding semilandmarks, a method developed by GREEN (1996) and BOOKSTEIN (1997) to address the issue of semilandmark interdependence and can allow for both landmarks and outlines to be used in an analysis.

In a study published by MOTT et al (2009), they assessed the use of digital image analyses for the application of traditional morphometrics in wildlife research. They used both calliper-based and digital image-based measurements on three life stages of the marbled salamander *Amblyostoma opacum* and found that the digital image-based measurements were significantly more accurate and faster to obtain compared to the calliper-based methods, as well as reducing their inter-observer measurement variation. However, they also concluded that digital-image results showed reduced precision in repeated measurements compared to the calliper-based results. They suggest that digital image-based morphometric methods are a useful alternative to handheld callipers, especially in situations where the specimen or organism cannot be analysed in a close proximity.

The study made by DRAKE et al. (2015) is an example of the application of 3D geometrics morphometric methods to analyse the previously studied canid skulls for which calliper-based morphometrics were used. They use bivariate plots of linear distances taken from dog and wolf skulls and Principal Component Analysis of cranial ratios to demonstrate an almost complete overlap between dogs and wolves, rendering these analyses unfit for classifying fossil

specimens as either dog or wolf. They concluded that the preservation of shape information and the inclusion of its variation in analyses is more accurately performed using Procrustes based geometric morphometrics and it aligned with the genetic testing that was performed on the analysed skulls. The information they gathered regarding the classification of the analysed skulls from various archaeological sites has disproven previous studies suggesting the time of domestication of dogs and they plan to continue applying these new methods on further collections in order to address the origin of domestication.

3. MATERIAL AND METHODS

Data collection

The skulls used in this study were provided by the Department of Anatomy, Histology and Embryology, University of Zagreb which feature in their pre-existing collection of anatomical specimens. 43 skulls were measured, of which 41 belonged to various breeds of dogs (*Canis lupus familiaris*) of known gender and age, and 2 were from wolves (*Canis lupus*). The dog breeds that were included in this study are depicted in Table 1.

Table 1: Dog breeds and respective sample size.

Dog Breed	Number of Skulls
Doberman Pincher	20
Crossbreed	6
Tornjak	5
Boxer	3
Dogo Argentino	1
Border terrier	1
Dalmatian	1
Terrier	1
Newfoundland	1
NA	2

NA= unknown breed

Traditional morphometrics

For the traditional (calliper-based) morphometric methods measurements were taken according to VON DEN DRIESCH (1976) (Figure 1-3). The common names and details of the measurements are shown in Table 2. Each of the 43 skulls was measured using the same analogue calliper for the total length of the skull (M1) and the same digital calliper for all other measurements.

From these 43 skulls, 9 representative skulls from each breed were chosen to be photographed from 3 different aspects (dorsal, ventral, and lateral). These images were used in the software MorphoJ (KLINGENBERG, 2011) for digital distance measurements. The measurements taken from the digital images were then used to calculate indices for each representative skull. Further to this, the same measurements used for the calliper-based methods were used for the digital images.

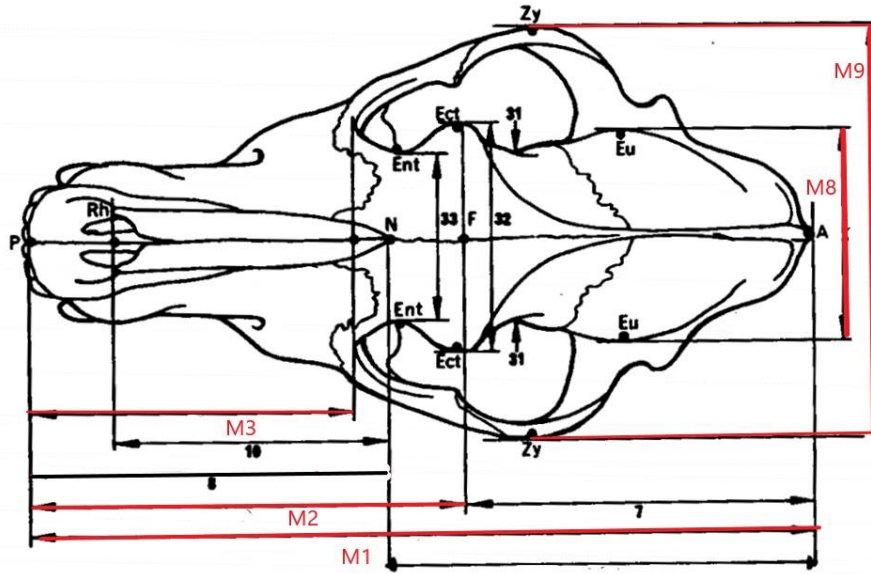


Figure 1. Dorsal aspect of dog skull with measurements by VON DEN DRIESCH (1976). The used measurements are marked in red.

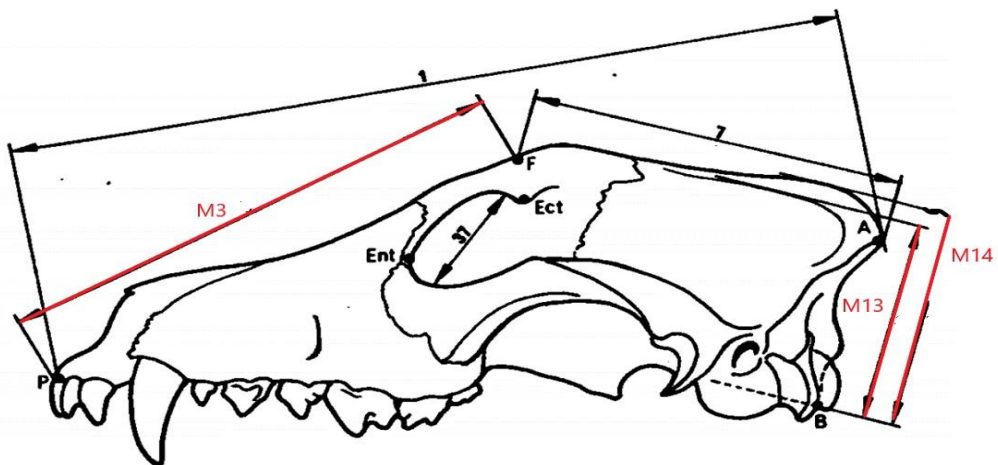


Figure 2. Lateral aspect of dog skull with measurements by VON DEN DRIESCH (1976). The used measurements are marked in red.

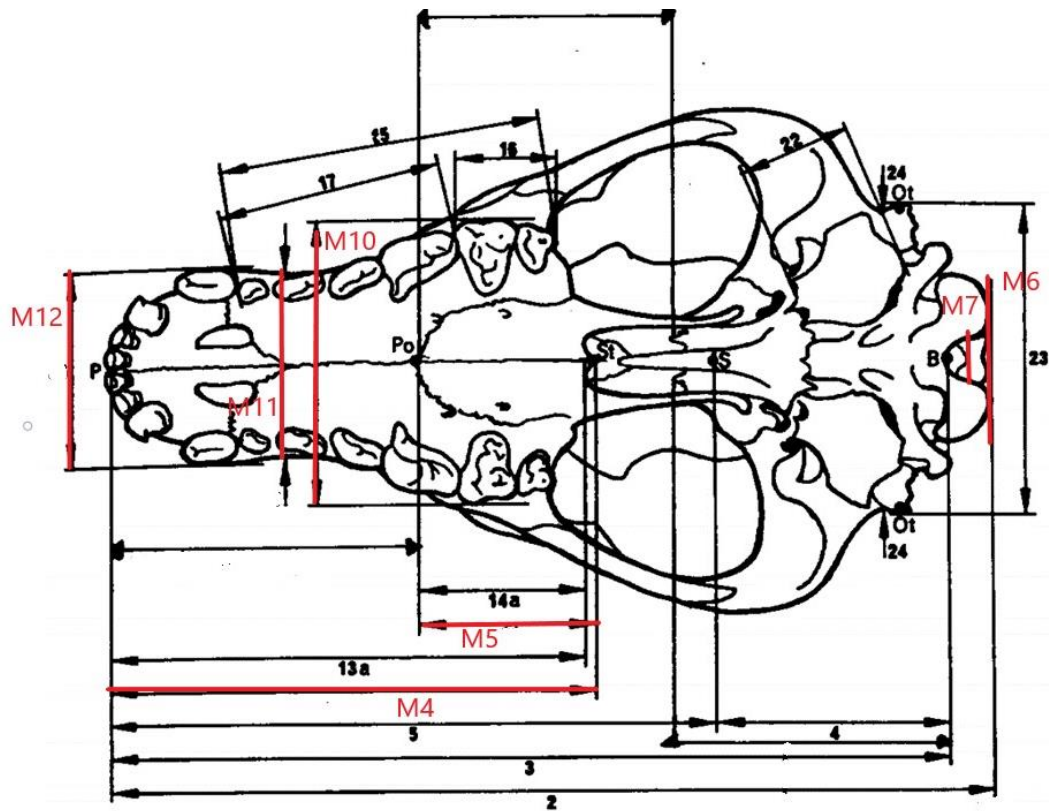


Figure 3. Ventral aspect of dog skull with measurements by VON DEN DRIESCH (1976). The used measurements are marked in red.

Geometric morphometrics

For the geometric morphometric methods, a Nikon D5300 digital camera was used to take images of the dorsal (Figure 4) ventral (Figure 5), and lateral aspect (Figure 6) of a representative skull from each breed of the same collection used for the calliper-based measurements. The images were taken from the same distance to the camera, including a ruler for scale. They were uploaded onto the tpsUtil and tpsDig2 programs for scaling and landmark determination. Following this, the coordinate data of the landmarks was uploaded to MorphoJ (KLINGENBERG, 2011) where a Procrustes superimposition was generated. Based on this, a Principal Component Analysis was performed for breed variance comparison.

Table 2. Measurements used in the study by VON DEN DRIESCH (1976) and their corresponding name and description.

Measurement number in study	Name of the measurement	Description of the measurement
M1	Total length	akrocranion → prosthion
M2	Facial length	frontal midpoint → prosthion
M3	“Snout” length	oral border of the orbits (median) → prosthion
M4	Palatal length	median palate length: staphylion → prosthion
M5	Horizontal palatal length	horizontal length of palatine (staphylion → palatinoorale)
M6	Occipital condyle breadth	greatest breadth of the occipital condyles
M7	Breadth of foramen magnum	greatest breadth of foramen magnum
M8	Cranial width	greatest breadth of the braincase, (greatest neurocranium width); euryon → euryon
M9	Zygomatic breadth	Zygion → Zygion
M10	Palatal width	greatest palatal breadth: molar → molar (measured across the outer borders of the alveoli)
M11	Least palatine breadth	least palatal breadth (measure behind canines)
M12	Breadth at canines	breadth at the canine alveoli
M13	Skull height	The two pointers of the calliper are placed basally on the basis of the skull and dorsally on the highest elevation of the sagittal crest
M14	Skull height without sagittal crest	Similar to M13; upper pointer is placed behind the sagittal crest

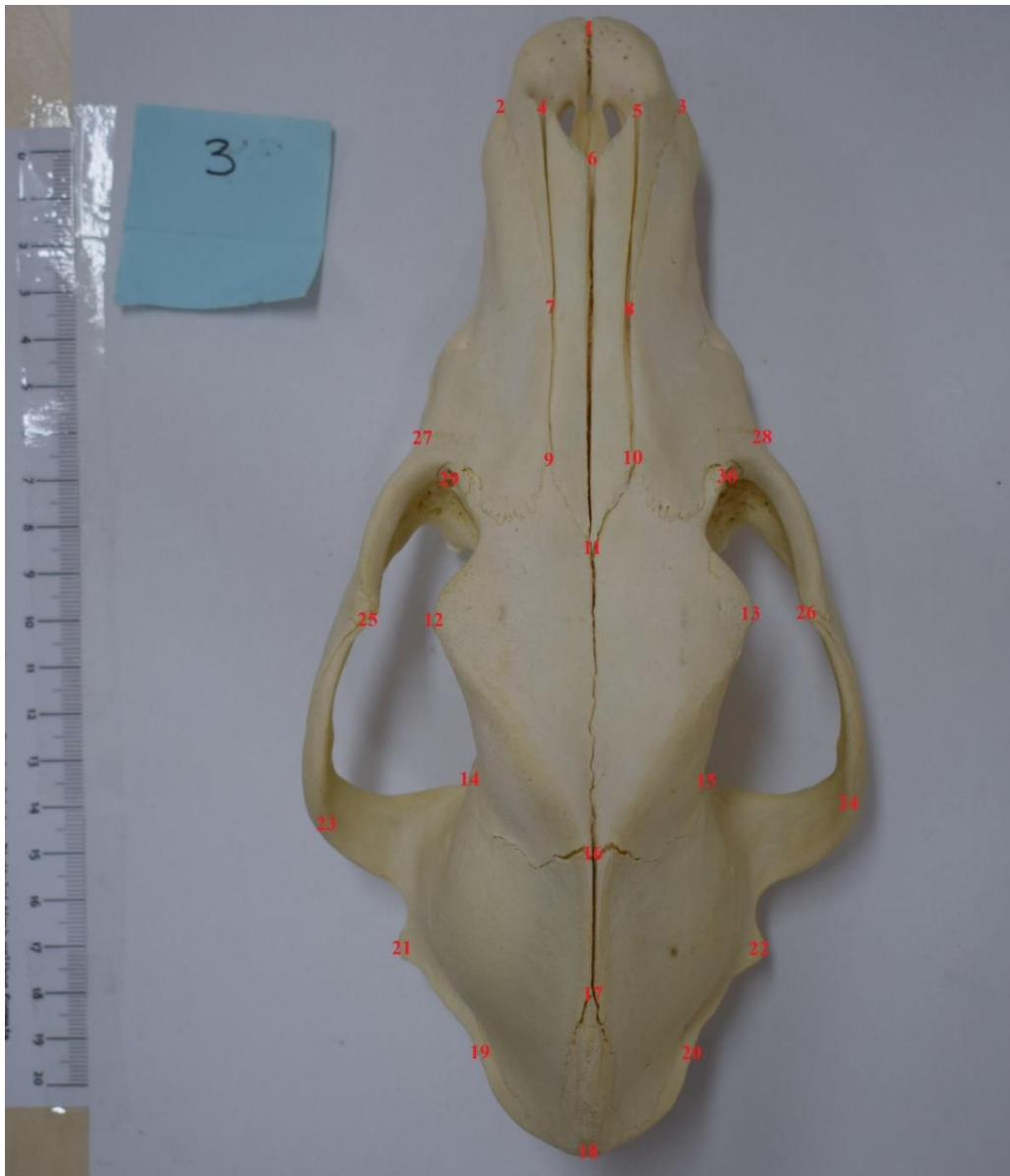


Figure 4. Dorsal aspect landmarks on Skull 3.

Table 3 presents the landmarks used for the dorsal aspect of each skull. The numbers correspond to the anatomical points on the skull presented in Figure 4 and the description for each point was taken from DRAKE et al. (2010).

Table 3: Landmark definitions for dorsal aspect.

Landmark	Description
1	Midline point on the premaxilla at the inferior tip of the bony septum between the upper central incisors
2	Premaxillary-maxillary suture, anterior, left side
3	Premaxillary-maxillary suture, anterior, right side
4	Nasal, anterior tip, left side
5	Nasal, anterior tip, right side
6	Nasale, nasal, anterior, midline
7	Premaxillary-maxillary suture, posterior end in dorsal view, left side
8	Premaxillary-maxillary suture, posterior end in dorsal view, right side
9	Frontal-maxillary-nasal suture, left side
10	Frontal-maxillary-nasal suture, right side
11	Nasion, nasal-frontal suture, midline
12	Zygomatic process of frontal bone, left side
13	Zygomatic process of frontal bone, right side
14	Frontal-parietal-sphenoid suture, left side
15	Frontal-parietal-sphenoid suture, right side
16	Bregma, frontal-parietal suture, midline
17	Lambda, parietal-occipital suture, midline
18	Opisthion, dorsal lip of foramen magnum, midline
19	Asterion, posterior at occipital-parietal-temporal suture, left side
20	Asterion, posterior at occipital-parietal-temporal suture, right side
21	External auditory meatus, posterior, left side
22	External auditory meatus, posterior, right side
23	Squamosal-jugal suture, posterior projection of jugal, ventral, left side
24	Squamosal-jugal suture, posterior projection of jugal, ventral, right side
25	Squamosal-jugal suture, anterior projection of zygomatic process of temporal bone, left side
26	Squamosal-jugal suture, anterior projection of zygomatic process of temporal bone, right side
27	Zygo-maxillare inferior, left side
28	Zygo-maxillare inferior, right side
29	Fossa lacrimalis, left side
30	Fossa lacrimalis, right side

Table 4 presents the landmarks used for the ventral aspect of each skull. The numbers correspond to the anatomical points on the skull presented in Figure 5 and the description for each point was taken from DRAKE et al. (2010).



Figure 5. Ventral aspect landmarks on Skull 3.

Table 4: Landmark definitions for ventral aspect.

Landmark	Description
1	Premaxillary-maxillary suture, lateral end in ventral view, left side
2	Premaxillary-maxillary suture, lateral end in ventral view, right side
3	Premaxillary-maxillary suture, posterior at midline
4	Premolar 4 (posterior buccal corner), right side
5	Premolar 4 (posterior buccal corner), left side
6	Maxillary-palatine suture, anterior at midline
7	Caudal to second molar, left side
8	Caudal to second molar, right side
9	Palatine, posterior at midline
10	Palatine-pterygoid suture posterior, right side
11	Palatine-pterygoid suture posterior, left side
12	Presphenoid, anterior tip at midline
13	Presphenoid-basisphenoid suture, midline
14	Optic canal (ventral lip), right side
15	Optic canal (ventral lip), left side
16	Basioccipital
17	Tympanooccipital fissure, anterior lip, right side
18	Tympanooccipital fissure, anterior lip, left side
19	Paracondylar process, right side
20	Paracondylar process, left side
21	Occipital condyle (widest point of foramen magnum), right side
22	Basion, ventral lip of foramen magnum, midline
23	Occipital condyle (widest point of foramen magnum), left side
24	Squamosal-jugal suture, posterior projection of jugal, ventral, right side
25	Squamosal-jugal suture, posterior projection of jugal, ventral, left side

Figure 6 shows Skull 3 as an example for lateral landmark representation. The numbers mark the landmark points and correspond to the landmarks in Table 5. The red lines depict the curves from landmarks 3-4, 5-6, 8-10-12, and 9-11.

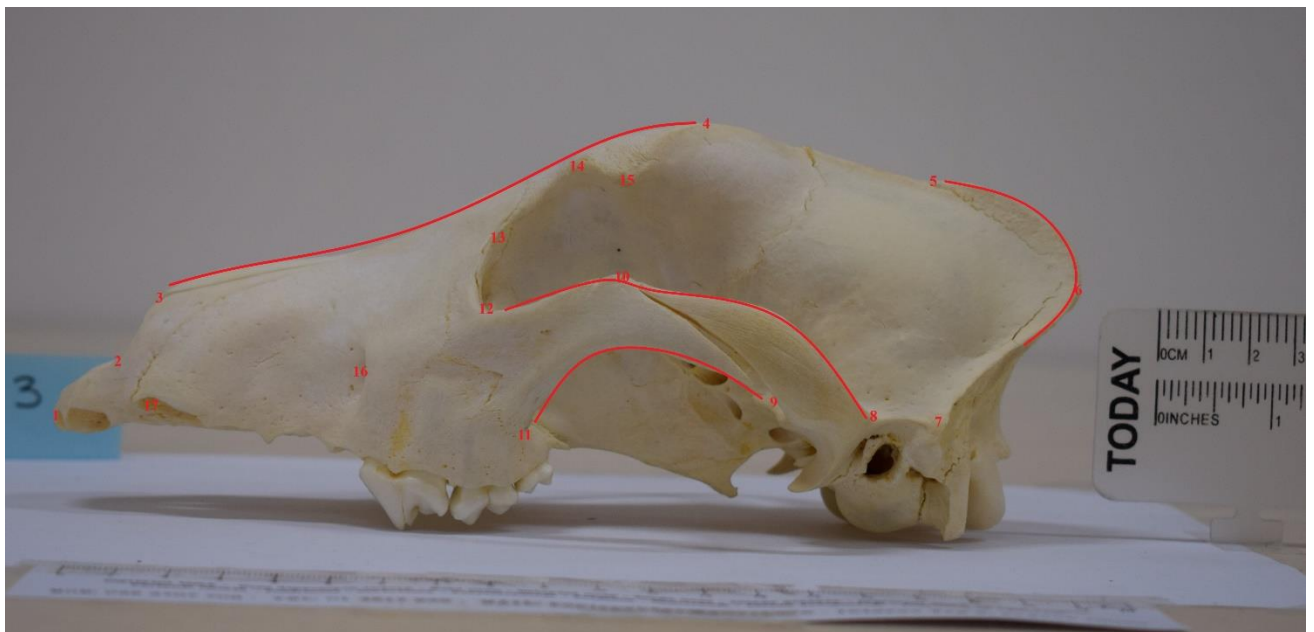


Figure 6. Lateral aspect landmarks on Skull 3.

Table 5 presents the landmarks used for the lateral aspect of each skull. The numbers correspond to the anatomical points on the skull presented in Figure 5 and the description for each point was taken from DRAKE et al. (2010).

Table 5: Landmark definitions for lateral aspect.

Landmark	Description
1	Midline point on the premaxilla at the inferior tip of the bony septum between the upper central incisors
2	Pseudolandmark – curve formed from incisive and nasal bones
3	Nasale, nasal, anterior, midline
4	Bregma, frontal-parietal suture, midline
5	Lambda, parietal-occipital suture, midline
6	Opisthion, dorsal lip of foramen magnum, midline
7	Pseudolandmark – lateral process caudal to origin of zygomatic process of temporal bone
8	Pseudolandmark – caudal part of origin of zygomatic process of temporal bone
9	Squamosal-jugal suture, posterior projection of jugal, ventral, left side
10	Squamosal-jugal suture, anterior projection of zygomatic process of temporal bone, left side
11	Pseudolandmark – ventral origin of zygomatic bone
12	Fossa lacrimalis – left side
13	Groove for angularis oculi vein
14	Pseudolandmark – anterior edge of the orbit
15	Zygomatic process of frontal bone – left side
16	Foramen infraorbitale – left side
17	Canine (anterior buccal corner), left side

Table 6 presents the indices that were calculated based on measurements taken from digital imaging software MorphoJ (KLINGENBERG, 2011). The indices were taken from EVANS and DE LAHUNTA (2013) and KOCH et al. (2012) with their respective calculation formulas.

Table 6: Indices and their calculation formulas.

Indices	Calculation of indices	Brachycephalic	Mesaticephalic	Dolichocephalic
Cranial index (CI) ^a	(CW x 100)/CL	57	56	48
Skull index (SI) ^a	(SW x 100)/SL	81	52	39
S-index (S-I) ^b	FL(DV)/CL(DV)*	-	-	-
Facial index (FI) ^a	(SW x 100)/FL	215	111	81
Palatal index (PI) ^a	(PW x 100)/PL	171-183***	-	60**

*DV-Dorsoventral View; **GSD - index for German Shephard Dog; *** Index range from English Bulldog to Brussels Griffon. CW - Cranial Width, CL - Cranial Length, SW - Skull Width, SL - Skull Length, FL - Facial Length, PW - Palatal Width, PL - Palatal Length.

^aEVANS, DE LAHUNTA (2013); ^bKOCH et al. (2012).

Statistical methods

The individual skull measurements contained in Microsoft Excel files, were input into SPSS Statistics software (IBM® SPSS® Statistics). Firstly, the data were tested for normality using the Shapiro-Wilk test and the measurements that were found to have normal distribution were used for one-way ANOVA testing. This involved comparing each dog breed to the measurements that were normally distributed.

4. RESULTS

Table 7 presents each individual dog skull that was measured with its respective breed, identification number and results corresponding to each measurement.

Table 7: Individual dog skull measurements and their respective breeds, for measurements M1-7.

Breed/Species	Skull ID	M1	M2	M3	M4	M5	M6	M7
Border Terrier	318	18	8.72	5.54	7.97	3.15	4.03	1.95
Boxer	161	17.5	9.9	6.95	8.37	2.8	3.61	1.9
Boxer	163	19.5	10.5	7.18	8.56	3.25	3.85	1.96
Boxer	164	19.4	11	7.68	8.8	3.11	3.84	1.84
Crossbreed	1	16.7	8.9	6.77	8.07	3.04	3.36	0.5
Crossbreed	68	18.8	10.32	7.42	9.05	3.36	3.65	0.5
Crossbreed	158	22.2	12.4	9.1	10.7	3.3	4	2.2
Crossbreed	158	22.5	14.17	10.6	10.85	3.36	4.21	2.14
Crossbreed	214	23.6	13.82	10.22	12.05	42.08	4.54	2.27
Crossbreed	304	19.4	11.6	8.2	9.88	3.28	3.29	1.84
Dalmatian	39	16.75	10.28	6.66	8.44	2.95	3.42	1.73
Doberman	90	25.65	14.51	11.39	12.5	3.82	4.36	2.21
Doberman	165	24.4	14.2	11.07	11.93	3.1	4.27	2.25
Doberman	166	22.7	14.1	9.9	11.5	3.3	4.5	1.7
Doberman	168	22.85	13.46	10.31	11.47	3.77	4.57	2.39
Doberman	169	22.8	13.09	10.12	11.41	3.72	4.25	2.18
Doberman	169	22.8	12.9	9.95	11.5	3.58	4.24	2.1
Doberman	170	22.9	13.75	10.56	11.13	3.8	4.22	2.06
Doberman	171	21.5	12.91	9.75	10.86	3.63	4.24	2.15
Doberman	172	24	14.33	10.6	12.03	3.87	4.18	2.08
Doberman	173	22.6	13.46	10.19	11.55	3.79	7.66	1.69
Doberman	174	22.45	13.28	10.39	11.49	3.48	4.05	2.12
Doberman	175	25.1	14.46	10.84	12.29	3.98	4.99	2.34
Doberman	176	24.9	14.57	11.26	12.03	4.13	4.56	2.18
Doberman	79-1	18.6	11.82	8.51	8.81	2.97	4.28	1.85
Doberman	79-2	23.1	13.74	10.5	12.02	4.38	4.38	2.37
Doberman	79-3	22.9	13.94	10.42	11.5	3.48	4.3	2.14
Doberman	79-5	20.95	12.84	9.34	10.46	3.38	4.08	2.1
Doberman	79-6	18.55	11.65	8.65	8.79	2.89	4.27	1.74
Doberman	79-9	25.2	14.6	11.39	12.1	3.96	4.53	2.25
Doberman	79-VANDA	22.5	13.6	10.41	10.99	3.6	4.2	2.2
Dogo Argentino	88	20.2	11	8.5	9.2	3.4	4.4	2.3
Newfoundland	307	22.37	12.98	9.58	11.08	3.75	4.28	2.05
Terrier	321	19.62	11.48	8.42	10	3.42	3.66	1.96
Tornjak	3	21.6	12.03	8.9	10.78	4.07	4.23	0.75
Tornjak	3	22.5	14.44	9.97	11.27	4.13	4.12	2.35
Tornjak	4	22.73	13	10.1	10.6	3.6	5.7	1.7
Tornjak	61	21.4	13.82	8.78	10.55	3.84	4.25	2.07
Tornjak	299	23.9	14.53	10.39	11.39	4.11	4.61	2.45
Wolf (<i>Canis lupus</i>)	udbima 11/1996 200/11	24.35	14.24	-	11.95	3.98	4.44	2.06
Wolf (<i>Canis lupus</i>)	Wolf	23.3	13.8	9.2	11.3	4	4.2	2.1
NA	159	22.3	-	11.7	11.95	3.96	4.35	2.25
NA	"A"	19.23	12.07	8.04	9.77	3.59	3.98	1.8

NA=unknown breed

Table 7: Continued for measurements M8-14.

Breed/Species	Skull ID	M8	M9	M10	M11	M12	M13	M14
Border Terrier	318	5.09	14.23	8.72	4.5	5.22	7.2	6.1
Boxer	161	5.76	11.53	7.78	4.18	4.38	6.2	5.8
Boxer	163	4.75	12.87	8.25	4.33	4.65	7.36	6.36
Boxer	164	5.44	12.74	8.41	4.62	4.64	7.06	6.8
Crossbreed	1	5.23	9.12	5.84	3.35	3.29	4.47	4.97
Crossbreed	68	5.3	10.23	6.14	3.27	3.53	6.04	5.24
Crossbreed	158	5.5	10.6	5.1	2.5	3.9	6.1	5.8
Crossbreed	158	5.08	10.21	6.57	3.44	3.83	6.11	5.13
Crossbreed	214	5.25	11.67	7.32	4.26	4.87	6.13	7.22
Crossbreed	304	5.36	9.12	6.5	3.78	4.02	5.97	5.46
Dalmatian	39	5.23	9.5	5.85	3.36	3.23	5.5	5.03
Doberman	90	5.34	11.31	7.07	3.74	4.21	7.35	5.75
Doberman	165	5.21	10.95	7.04	3.88	4.5	6.93	5.78
Doberman	166	5.8	10.9	5.5	2.5	4	7	6.5
Doberman	168	4.64	10.18	6.47	3.28	3.59	6.59	5.63
Doberman	169	5.17	11.03	6.52	2.86	3.65	6.6	5.69
Doberman	169	5.17	11.05	6.53	2.83	3.64	5.36	6.63
Doberman	170	5.5	10.23	6.46	3.49	3.64	6.48	5.86
Doberman	171	5.43	9.65	6.32	3.53	3.66	6.1	5.67
Doberman	172	5.67	11.11	6.9	3.5	4.01	7.28	5.86
Doberman	173	5.48	10.28	6.66	3.6	3.85	6.45	5.28
Doberman	174	4.92	10.37	6.58	3.35	3.71	6.33	5.43
Doberman	175	4.9	12.08	7.44	3.97	4.44	7.65	5.96
Doberman	176	4.75	11.32	7.25	3.52	4.11	7.23	5.76
Doberman	79-1	5.36	8.3	6.25	3.52	3.62	5.54	5.51
Doberman	79-2	4.96	11.54	7.75	4.3	4.47	6.77	5.69
Doberman	79-3	4.57	10.4	6.57	3.13	3.65	6.58	5.56
Doberman	79-5	4.92	9.21	5.92	3.11	3.47	6.01	5.57
Doberman	79-6	5.12	8.5	6.24	3.5	3.64	5.54	5.2
Doberman	79-9	4.88	11.5	6.78	3.26	3.9	7.18	5.8
Doberman	79-VANDA	4.74	-	6.58	3.25	3.68	6.88	5.84
Dogo Argentino	88	6.4	12.6	6.3	3.2	4.4	7.2	6.5
Newfoundland	307	-	10.12	6.24	2.98	3.38	-	-
Terrier	321	5.06	9.97	6.38	3.31	3.53	6.21	5.6
Tornjak	3	5.12	10.94	7.36	4.18	4.56	7.43	6.08
Tornjak	3	5.57	10.73	6.64	3.42	3.7	6.17	5.44
Tornjak	4	5.83	10.77	7	4.2	4.35	7.1	6.22
Tornjak	61	5.66	10.86	6.84	4.16	4.4	7.13	6.35
Tornjak	299	5.5	11	5.5	3.3	3	7.2	6.9
Wolf (<i>Canis lupus</i>)	udbima 11/1996 200/11	5.63	10.67	6.63	4.17	4.23	6.78	6.21
Wolf (<i>Canis lupus</i>)	Wolf	5.98	11.46	7.27	3.93	4.28	7.66	6.56
NA	159	6.3	13.76	8.2	4.23	4.56	7.16	6.28
NA	"A"	6.7	13.4	6.6	3	4.3	7.1	6.4

Table 8 depicts the representative skulls from each breed which were used for digital image measurements with the respective measurements needed for index calculation.

Table 8: Measurements made from digital images for the purpose of index calculations.

Breed	Skull ID	Skull Length	Skull Width	Cranial Length	Cranial Width	Facial Length	Facial Width	Palatal Width	Palatal Length
Border Terrier	318	19.54	15.57	11.68	6.42	7.77	15.57	9.44	9.37
Boxer	164	21.5	13.87	12.29	7.28	9.21	13.87	8.41	10.18
Crossbreed	68	20.99	11.55	10.97	6.32	9.77	11.55	6.45	11.39
Dalmatian	39	25.04	10.5	9.36	5.76	8.6	10.5	5.34	8.93
Doberman	90	28.23	13.12	15.53	6.25	12.7	13.12	6.7	14.75
Dogo Argentino	88	21.37	13.68	12.13	6.76	9.24	13.68	7.33	10.2
Newfoundland	307	22.23	10.87	11.91	6.11	10.29	10.87	7.32	13.6
Tornjak	3	23.66	11.8	12.6	6.42	10.86	11.8	6.72	13.4
Wolf	udbima 11/1996 200/11	28.65	16.25	15.66	8.08	13.22	16.25	7.93	13.52

Table 9 depicts the representative skulls from each breed which were used for digital image measurements with the respective index calculation result.

Table 9: Indices calculated from digital image-based measurements.

Breed	Skull ID	Cranial Index (CI)	Skull Index (SI)	S-Index	Facial Index (FI)	Palatal Index (PI)
Border Terrier	318	54.9	79.68	0.67	200	100.7
Boxer	164	59.23	64.5	0.74	150.6	82.6
Crossbreed	68	57.61	55.02	0.89	118.2	56.62
Dalmatian	39	61.53	41.93	0.92	122	59.8
Doberman	90	40.24	46.47	0.82	103	45.42
Dogo Argentino	88	55.72	64.01	0.76	148	71.86
Newfoundland	307	51.3	48.89	0.86	105.6	53.8
Tornjak	3	50.95	49.87	0.86	108.65	50.15
Wolf	udbima 11/1996 200/11	51.59	56.7	0.84	123	58.65

Table 10 depicts the measurements taken on the digital images of the representative skulls of each breed using the same measurements as for the calliper-based measurements.

Table 10: Digital image-based measurements of representative skulls.

Breed	Skull ID	Total Length M1	Facial Length M2	Snout Length M3	Palatal Length M4	Staphylion to Palatinoorale M5	Occipital Condyle Breadth M6	Foramen Magnum M7
Border Terrier	318	19.54	7.77	9.08	9.37	3.42	4.23	2.29
Boxer	164	21.5	9.21	9.33	10.18	3.57	4.3	1.96
Crossbreed	68	20.99	9.77	10.31	11.39	3.82	4.29	2.11
Dalmatian	39	25.04	8.6	9.72	8.93	3.32	3.64	1.62
Doberman	90	28.23	12.7	14.51	14.75	3.97	5.11	2.05
Dogo Argentino	88	21.37	9.24	11.06	10.2	3.41	4.23	2.08
Newfoundland	307	22.23	10.29	12.67	13.6	4.02	4.62	1.81
Tornjak	3	23.66	10.86	12.79	13.4	4.56	4.51	1.94
Wolf	udbima 11/1996 200/11	28.65	13.22	14.52	13.52	4.35	4.72	2.35
Breed	Skull ID	Cranial Width M8	Zygomatic Breadth M9	Palatal Width M10	Least Palatine Breadth M11	Breadth at Canines M12	Skull Height M13	Skull Height Without Crest M14
Border Terrier	318	6.42	15.57	9.44	5.01	5.73	7.21	6.89
Boxer	164	7.28	13.87	8.41	5.42	5.59	7.26	6.42
Crossbreed	68	6.32	11.55	6.45	3.86	4.18	6.84	6.03
Dalmatian	39	5.76	10.5	5.34	3.68	3.77	6.29	5.67
Doberman	90	6.25	13.12	6.7	4.48	5.11	7.86	6.47
Dogo Argentino	88	6.76	13.68	7.33	4.52	4.64	7.9	6.9
Newfoundland	307	6.11	10.87	7.32	4.8	5.12	8.1	7.25
Tornjak	3	6.42	11.8	6.72	4.47	4.75	7.55	6.79
Wolf	udbima 11/1996 200/11	8.08	16.25	7.93	4.58	5.04	8.03	7.01

Table 11 depicts the results from the statistical tests used for normality testing. The data used were all the measurements taken from each skull (presented in Table 7).

Table 11: Results from tests of normality and distribution. Statistic indicating test statistic, df as degrees of freedom. Asterisks indicating level of significance and ns non-significance.

Measurement	Kolmogorov-Smirnov				Shapiro-Wilk			
	Statistic	df	p-value	Significance	Statistic	df	p-value	Significance
Acromion-Prosthion	0.190	32	0.005	**	0.944	32	0.095	ns
Facial Length	0.172	32	0.017	*	0.892	32	0.004	**
Snout Length	0.184	32	0.007	**	0.91	32	0.011	*
Median Palate	0.169	32	0.021	*	0.888	32	0.003	**
Horizontal Palate	0.491	32	<0.001	***	0.218	32	<0.001	***
Occipital Condyle	0.261	32	<0.002	***	0.637	32	<0.002	***
Foramen Magnum	0.101	32	0.200	ns	0.971	32	0.523	ns
Brain Case	0.059	32	0.200	ns	0.989	32	0.981	ns
Zygomastics	0.118	32	0.200	ns	0.972	32	0.545	ns
Palatal Breadth	0.175	32	0.014	*	0.918	32	0.018	*
Least Palatal	0.162	32	0.031	*	0.962	32	0.305	ns
Alveoli Breadth	0.165	32	0.027	*	0.945	32	0.103	ns
Skull Height	0.107	32	0.200	ns	0.958	32	0.245	ns
Skull Height (No Crest)	0.169	32	0.021	*	0.944	32	0.095	ns

Figure 7 shows the graphically represented results of the one-way ANOVA for the measurement M1 (Total length of skull). The range of the data is 7.075, with the highest value being 23.825 for the Wolf, and the lowest 16.750 for the Dalmatian dog breed.

The P value for this measurement as a result of the ANOVA was $p < 0.05$ ($p = 0.005$), therefore I can conclude that the result is significant (there are significant differences between breeds for this measurement).

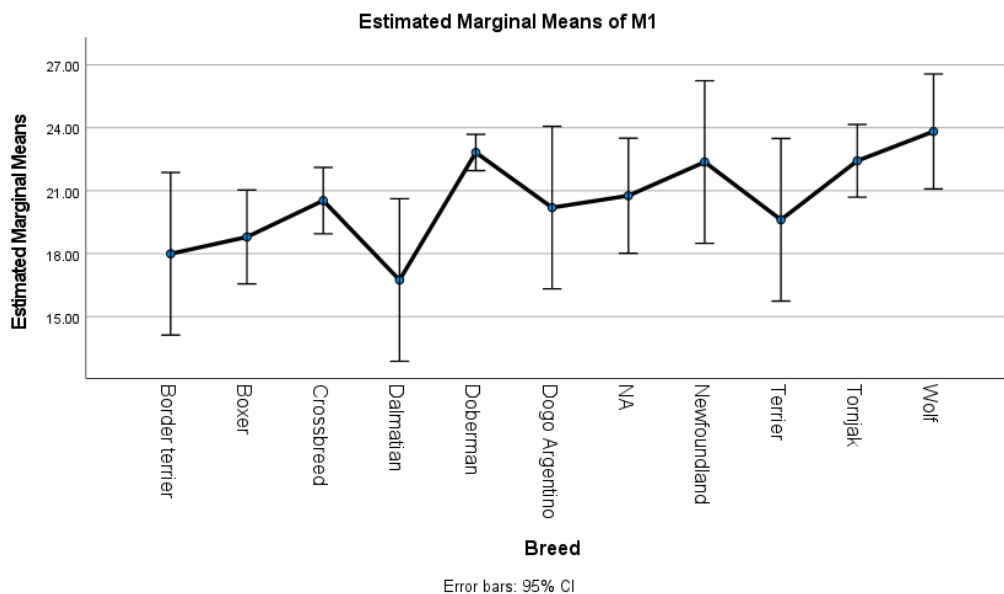


Figure 7. One-way ANOVA test results from the comparison of the measurements for M1 (Total length of skull) to each dog breed in the sample.

Figure 8 shows the graphically represented results of the one-way ANOVA for the measurement M7 (Breadth of foramen magnum). The range of the data is 0.725, with the highest value being 2.300 for the Dogo Argentino dog breed, and the lowest 1.575 for the Crossbreed dog breed.

The P value for this measurement as a result of the ANOVA was $p > 0.05$ ($p = 0.640$), therefore I can conclude that the result is not significant (there are no significant differences between breeds for this measurement).

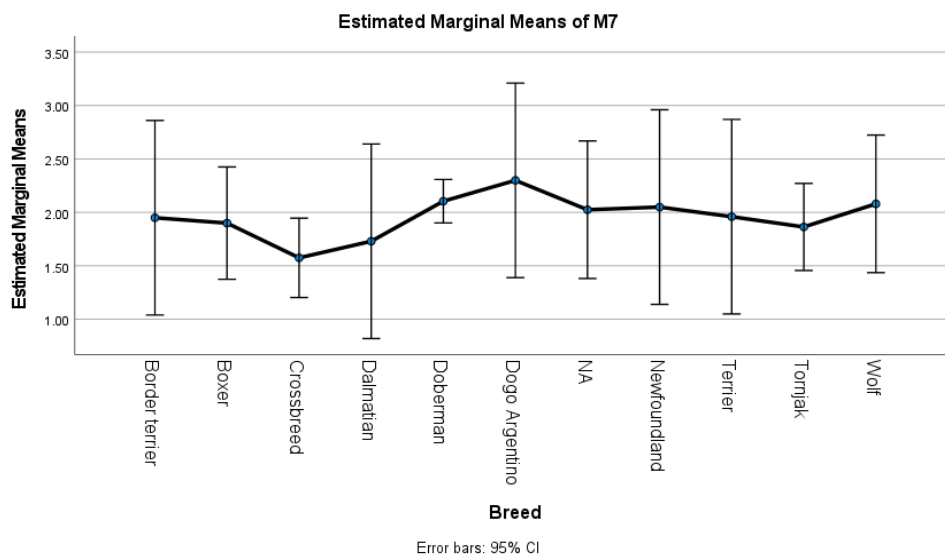


Figure 8. One-way ANOVA test results from the comparison of the measurements for M7 (Breadth of Foramen magnum) to each dog breed in the sample.

Figure 9 shows the graphically represented results of the one-way ANOVA for the measurement M8 (Greatest breadth of the braincase). The range of the data is 1.44, with the highest value being 6.500 for the Wolf, and the lowest 5.060 for the unknown (NA) dog breed. The P value for this measurement as a result of the ANOVA was $p < 0.05$ ($p < 0.001$), therefore I can conclude that the result is significant (there are significant differences between breeds for this measurement).

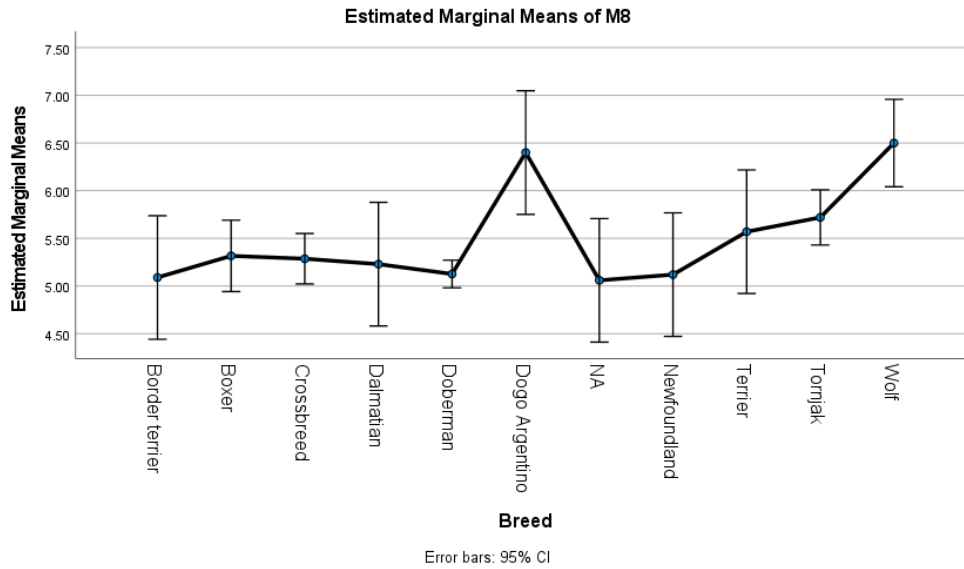


Figure 9. One-way ANOVA test results from the comparison of the measurements for M8 (Greatest breadth of braincase) to each dog breed in the sample.

Figure 10 shows the graphically represented results of the one-way ANOVA for the measurement M9 (Zygomatic breadth). The range of the data is 4.730, with the highest value being 14.230 for the Border terrier breed, and the lowest 9.500 for the Dalmatian breed. The P value for this measurement as a result of the ANOVA was $p < 0.05$ ($p < 0.001$), therefore I can conclude that the result is significant (there are significant differences between breeds for this measurement).

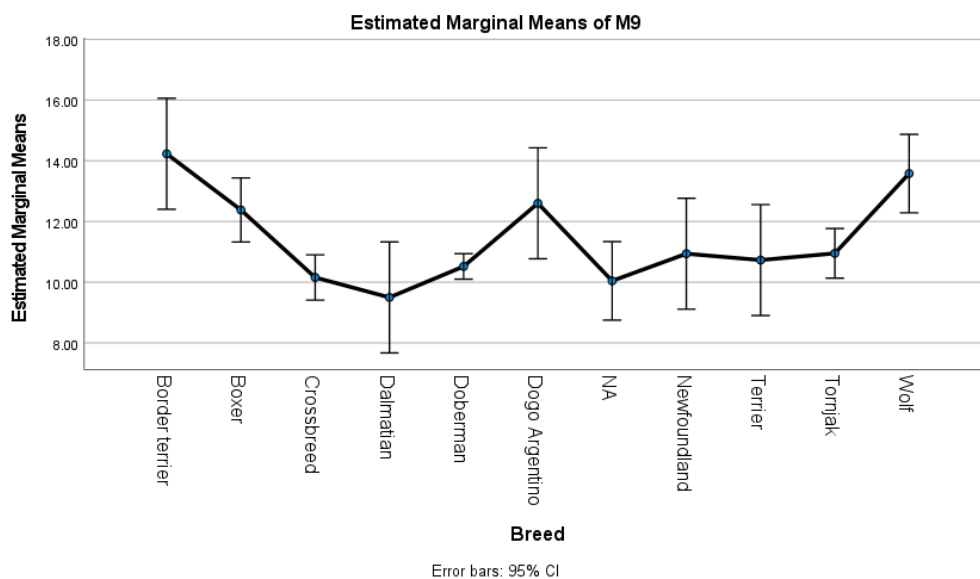


Figure 10. One-way ANOVA test results from the comparison of the measurements for M9 (Zygomatic breadth). to each dog breed in the sample.

Figure 11 shows the graphically represented results of the one-way ANOVA for the measurement M11 (Least palatal breadth (measure behind canines)). The range of the data is 1.355, with the highest value being 4.500 for the Border terrier dog breed, and the lowest 3.145 for the unknown (NA) dog breed.

The P value for this measurement as a result of the ANOVA was $p < 0.05$ ($p = 0.021$), therefore I can conclude that the result is significant (there are significant differences between breeds for this measurement).

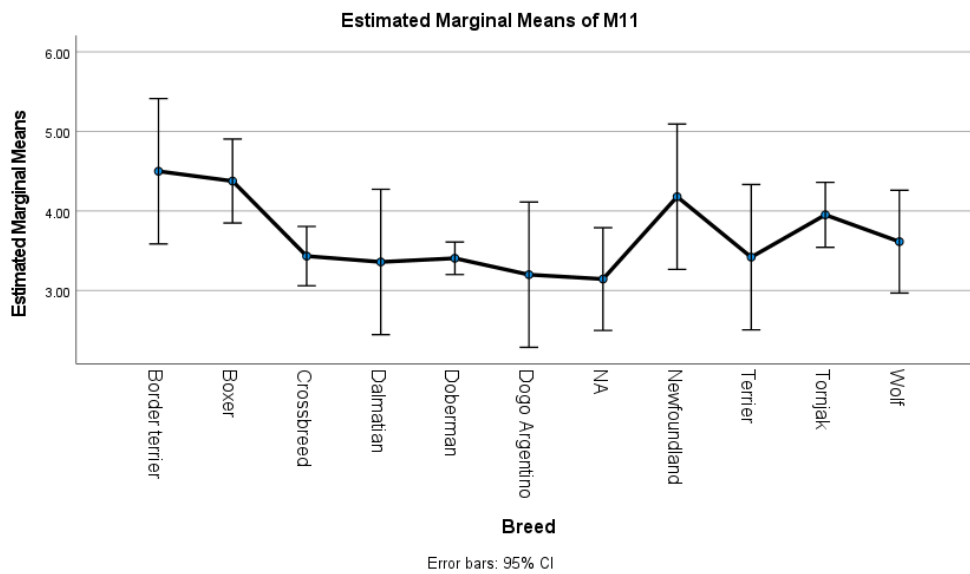


Figure 11. One-way ANOVA test results from the comparison of the measurements for M11 (Least palatal breadth (measure behind canines)) to each dog breed in the sample.

Figure 12 shows the graphically represented results of the one-way ANOVA for the measurement M12 (Breadth at the canine alveoli). The range of the data is 1.990, with the highest value being 5.220 for the Border terrier dog breed, and the lowest 3.230 for the Dalmatian dog breed.

The P value for this measurement as a result of the ANOVA was $p < 0.05$ ($p = 0.006$), therefore I can conclude that the result is significant (there are significant differences between breeds for this measurement).

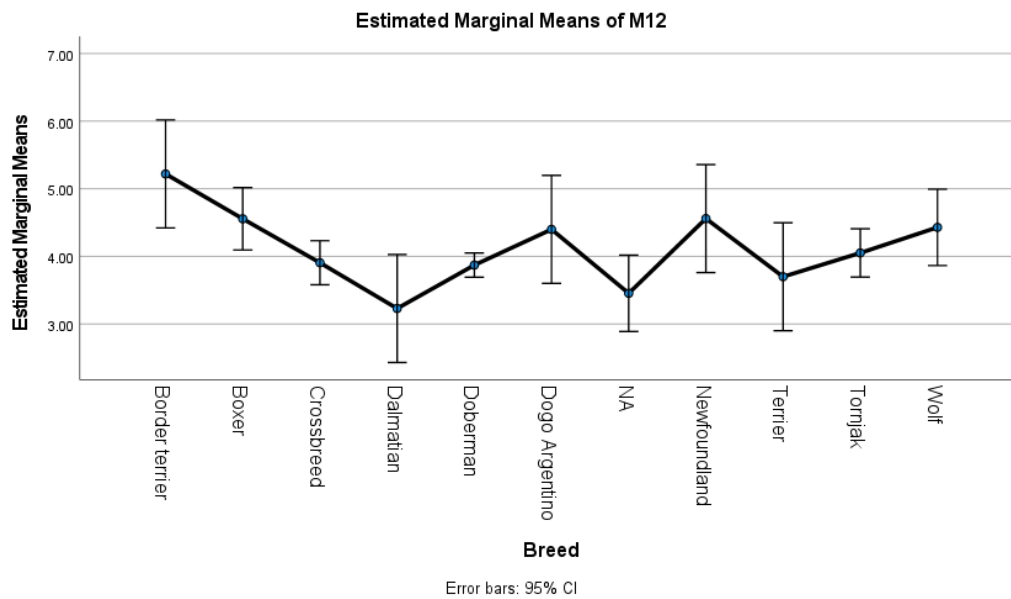


Figure 12. One-way ANOVA test results from the comparison of the measurements for M12 (Breadth at the canine alveoli) to each dog breed in the sample.

Figure 13 shows the graphically represented results of the one-way ANOVA for the measurement M13 (Skull height). The range of the data is 1.93, with the highest value being 7.430 for the Newfoundland dog breed, and the lowest 5.500 for the Dalmatian dog breed.

The P value for this measurement as a result of the ANOVA was $p < 0.05$ ($p = 0.021$), therefore I can conclude that the result is significant (there are significant differences between breeds for this measurement).

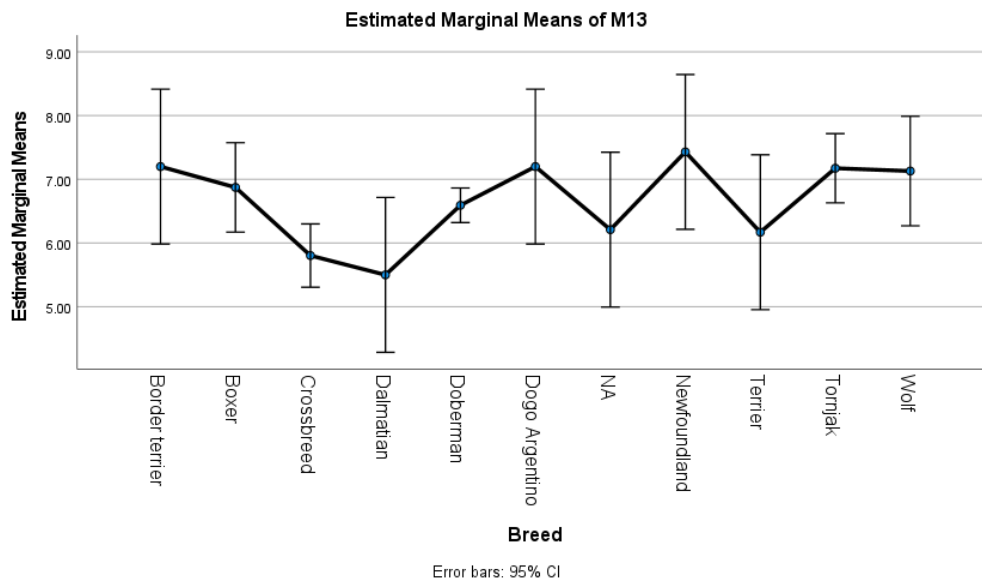


Figure 13. One-way ANOVA test results from the comparison of the measurements for M13 (Skull height) to each dog breed in the sample.

Figure 14 shows the graphically represented results of the one-way ANOVA for the measurement M14 (Skull height without sagittal crest). The range of the data is 1.47, with the highest value being 6.500 for the Dogo Argentino dog breed, and the lowest 5.030 for the Dalmatian dog breed.

The P value for this measurement as a result of the ANOVA was $p < 0.05$ ($p = 0.038$), therefore I can conclude that the result is significant (there are significant differences between breeds for this measurement).

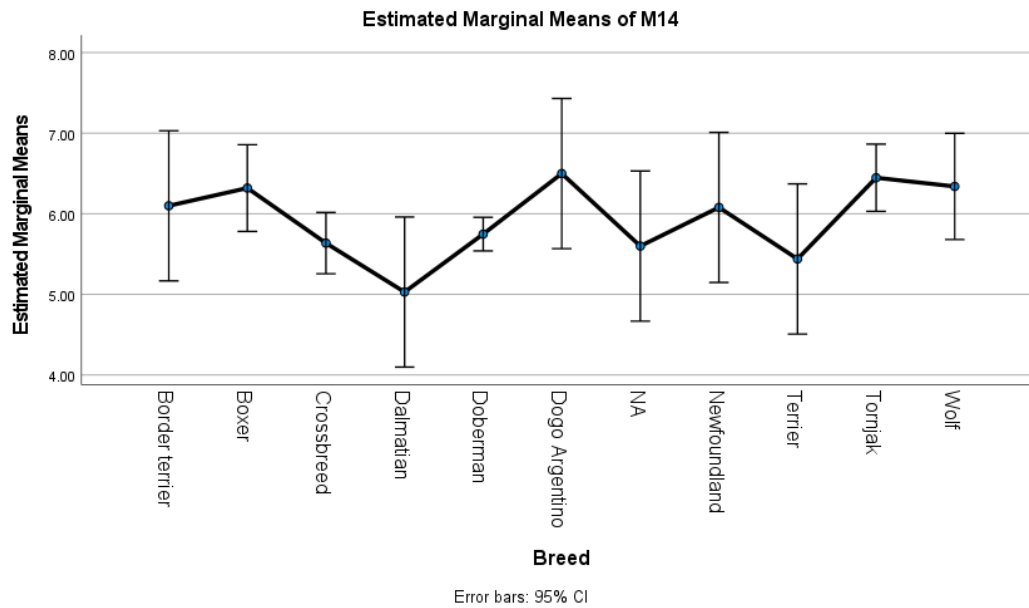


Figure 14. One-way ANOVA test results from the comparison of the measurements for M14 (Skull height without sagittal crest) to each dog breed in the sample.

Figure 15 is an example of a Procrustes superimposition of landmarks. In this figure, the landmarks from the ventral aspect of each dog skull were superimposed in the software MorphoJ which generated a mean for each landmark represented as the larger, bold, dark blue point with its corresponding number. The smaller points surrounding each larger point represent the landmarks from each dog skull. It was not possible to present in this figure which point corresponds to the respective breed.

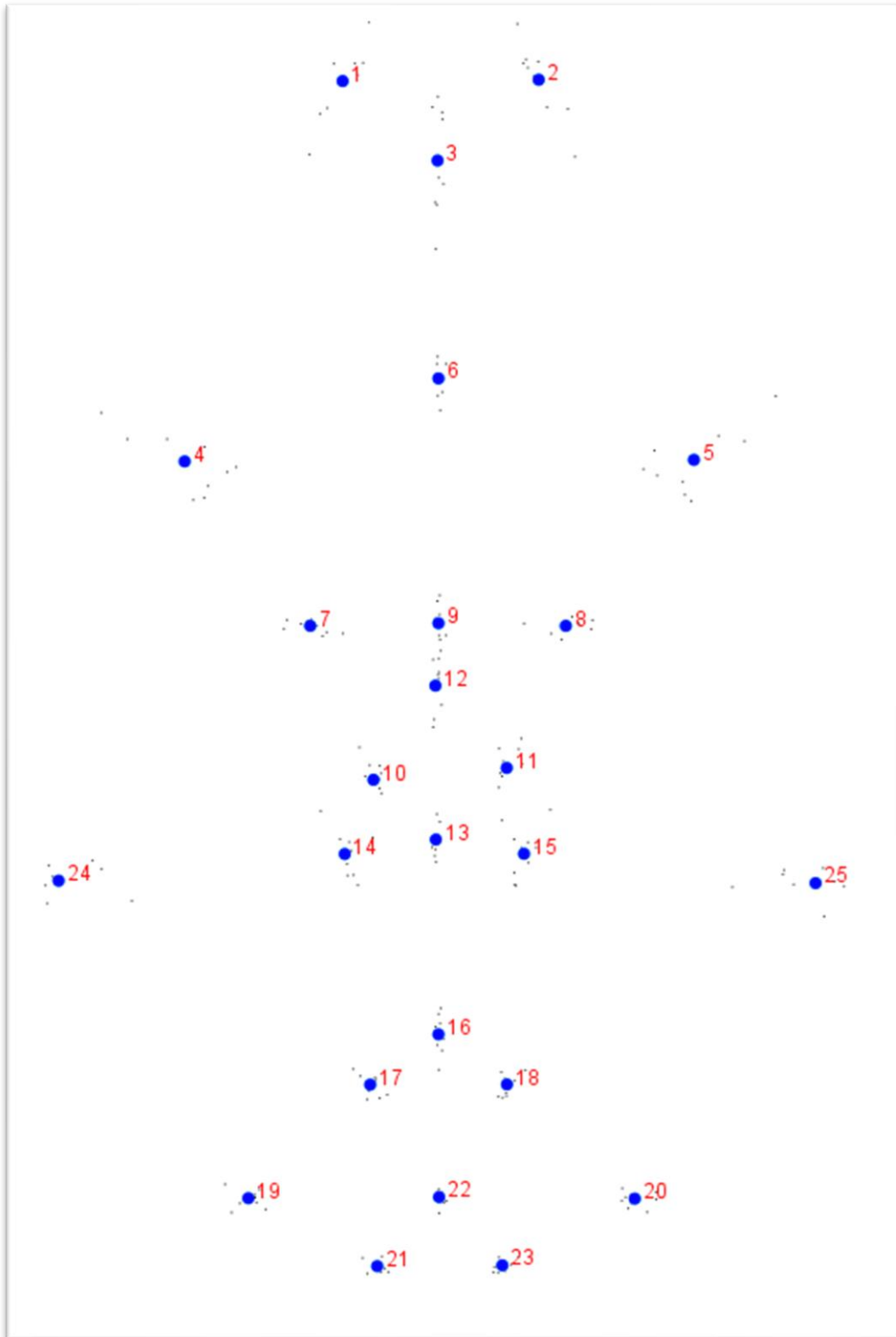


Figure 15. Example of a Procrustes superimposition. Procrustes analysis of the ventral aspect landmarks of each dog skull in the sample.

Figure 16 is a graphical representation of a Principal Component Analysis comparing the dorsal landmark results of each dog breed against the first and second Principal Components (Principal Component 1 vs Principal Component 2).

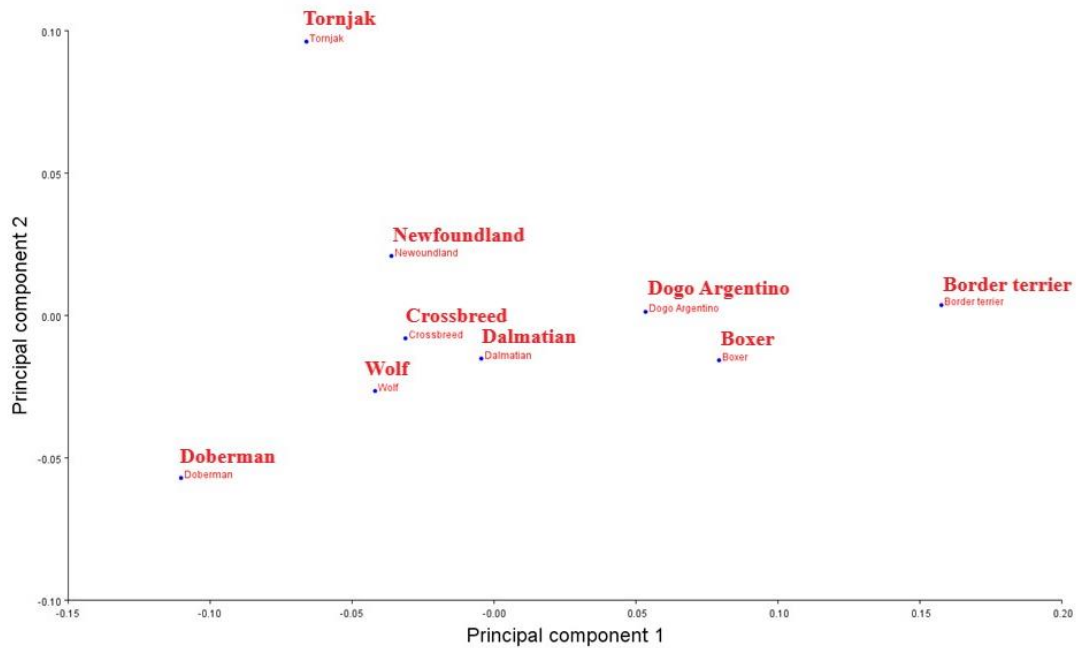


Figure 16. Graphical representation of the results from comparing Principle Component 1 to Principle Component 2 of the dorsal aspect landmarks.

Figure 17 is a wireframe graph of the dorsal aspect landmarks from the skull of the Border terrier (dark blue) superimposed with the mean dorsal aspect landmarks (light blue) from all the skulls used in the Procrustes analysis.

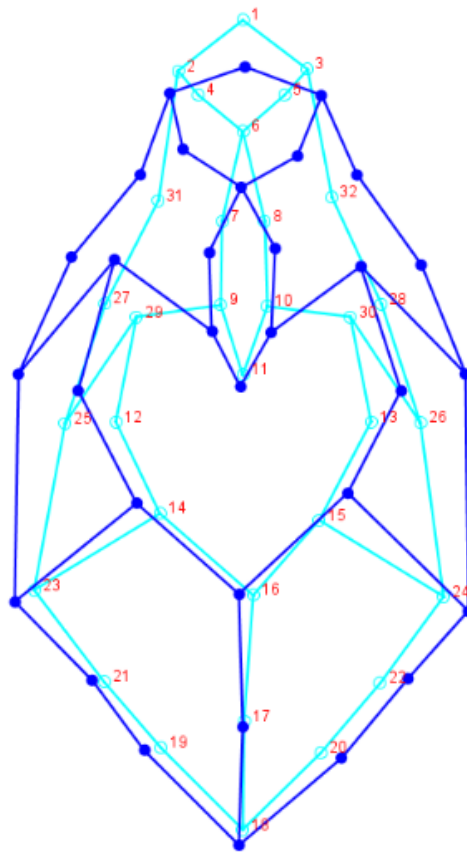


Figure 17. Wireframe comparison of dorsal landmarks from the Border terrier dog breed (dark blue) and the mean dorsal landmarks (light blue).

Figure 18 is a wireframe graph of the dorsal aspect landmarks from the skull of the Doberman dog breed superimposed with the mean dorsal aspect landmarks from all the skulls used in the Procrustes analysis.

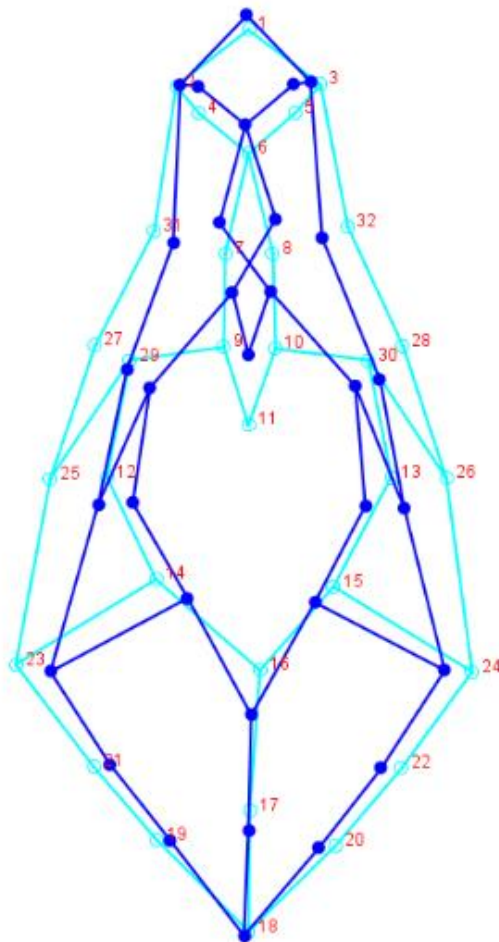


Figure 18. Wireframe comparison of dorsal landmarks from the Doberman dog breed (dark blue) and the mean dorsal landmarks (light blue).

Figure 19 is a wireframe graph of the dorsal aspect landmarks from the skull of the Dalmatian dog breed superimposed with the mean dorsal aspect landmarks from all the skulls used in the Procrustes analysis.

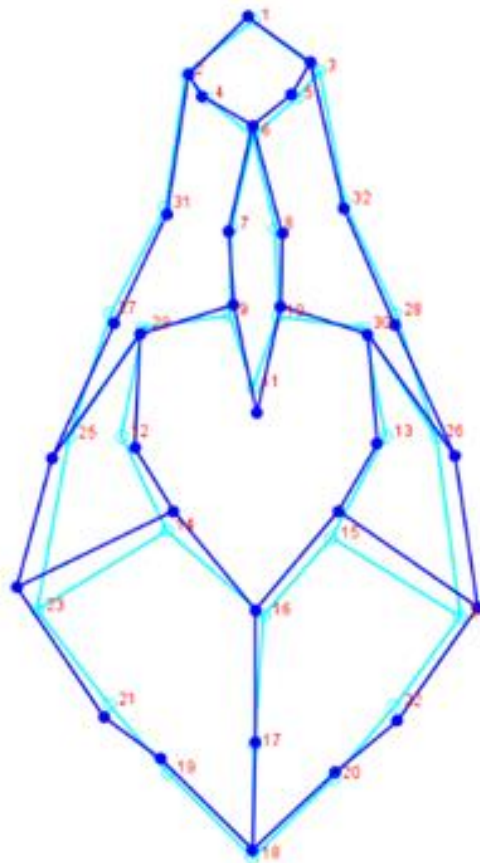


Figure 19. Wireframe comparison of dorsal landmarks from the Dalmatian dog breed (dark blue) and the mean dorsal landmarks (light blue).

Figure 20 is a graphical representation of a Principal Component Analysis comparing the lateral landmark results of each dog breed against the first and second Principal Components (Principal Component 1 vs Principal Component 2).

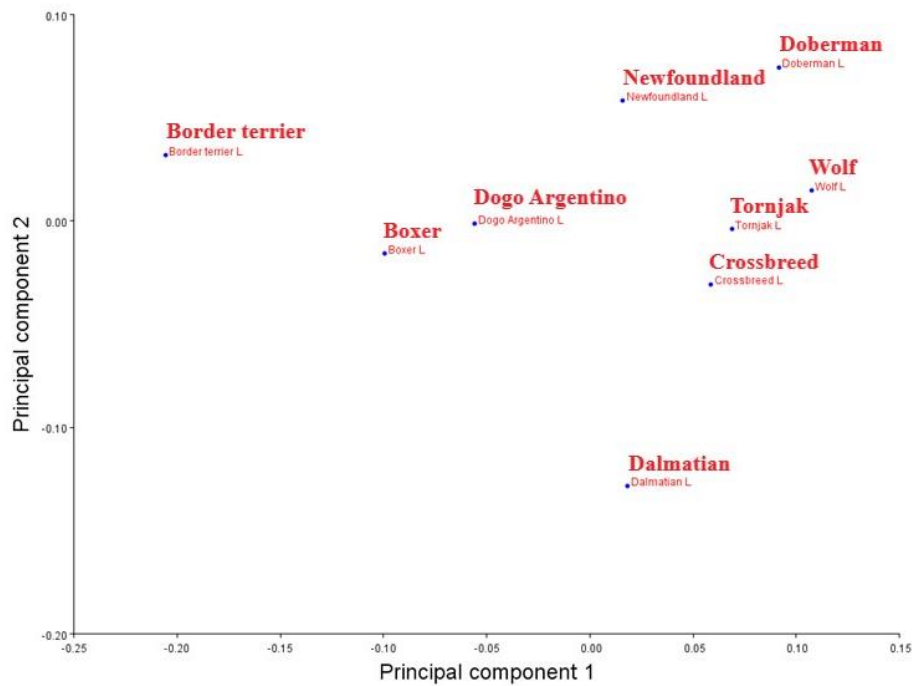


Figure 20. Graphical representation of the results from comparing Principle Component 1 vs Principle Component 2 of the lateral aspect landmarks.

Figure 21 is a wireframe graph of the lateral aspect landmarks from the skull of the Border terrier dog breed superimposed with the mean lateral aspect landmarks from all the skulls used in the Procrustes analysis.

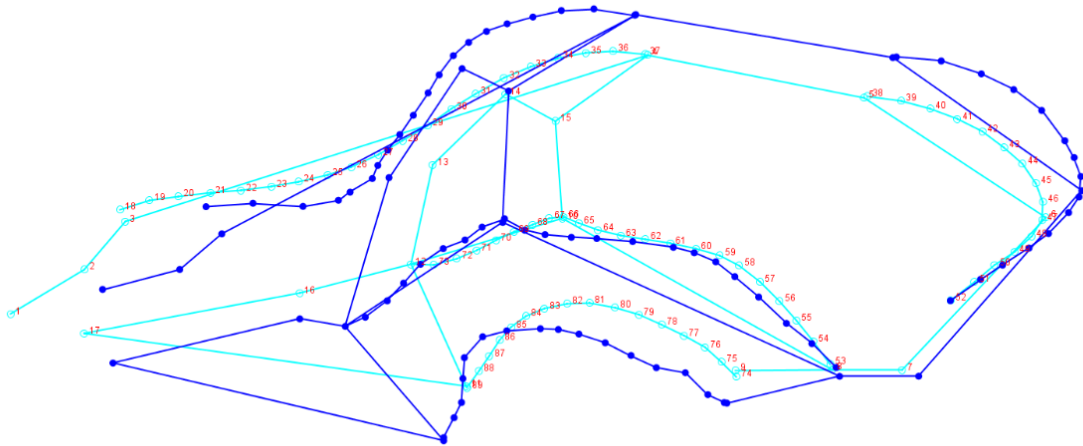


Figure 21. Wireframe comparison of lateral landmarks from the Border terrier dog breed (dark blue) and the mean lateral landmarks (light blue).

Figure 22 is a wireframe graph of the lateral aspect landmarks from the skull of the Doberman dog breed superimposed with the mean lateral aspect landmarks from all the skulls used in the Procrustes analysis.

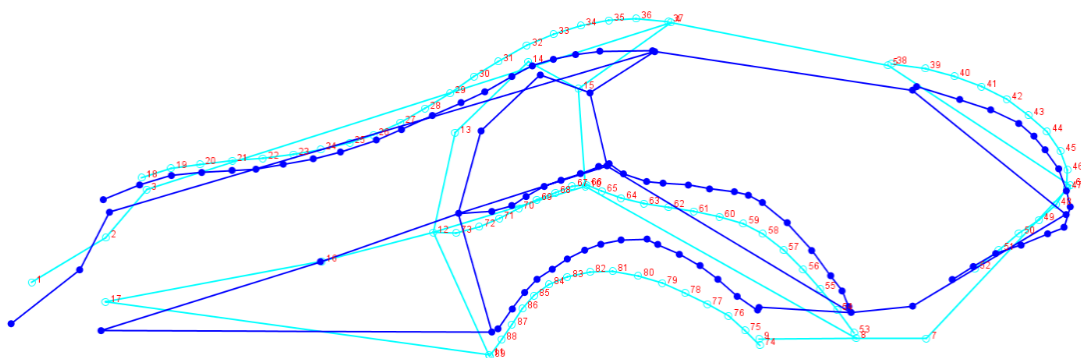


Figure 22. Wireframe comparison of lateral landmarks from the Doberman dog breed (dark blue) and the mean lateral landmarks (light blue).

Figure 23 is a wireframe graph of the lateral aspect landmarks from the skull of the Newfoundland dog breed superimposed with the mean lateral aspect landmarks from all the skulls used in the Procrustes analysis.

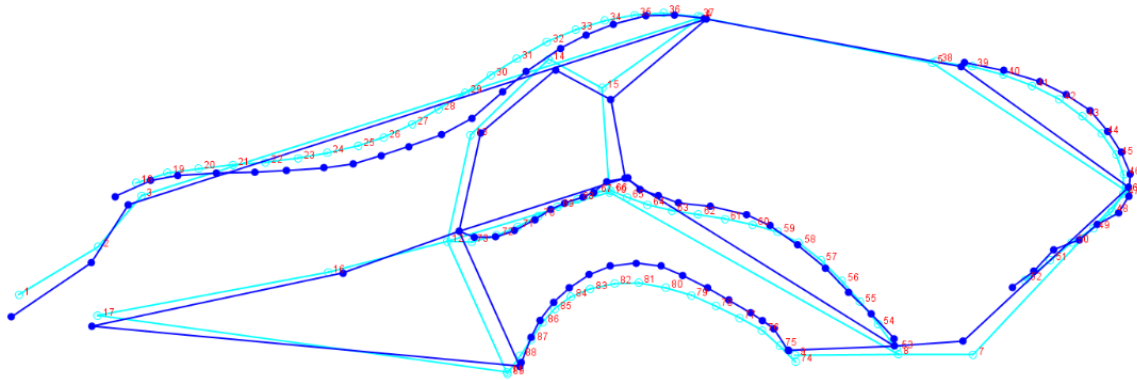


Figure 23. Wireframe comparison of lateral landmarks from the Newfoundland dog breed (dark blue) and the mean lateral landmarks (light blue).

Figure 25 is a graphical representation of a Principal Component Analysis comparing the ventral landmark results of each dog breed against the first and second Principal Components (Principal Component 1 vs Principal Component 2).

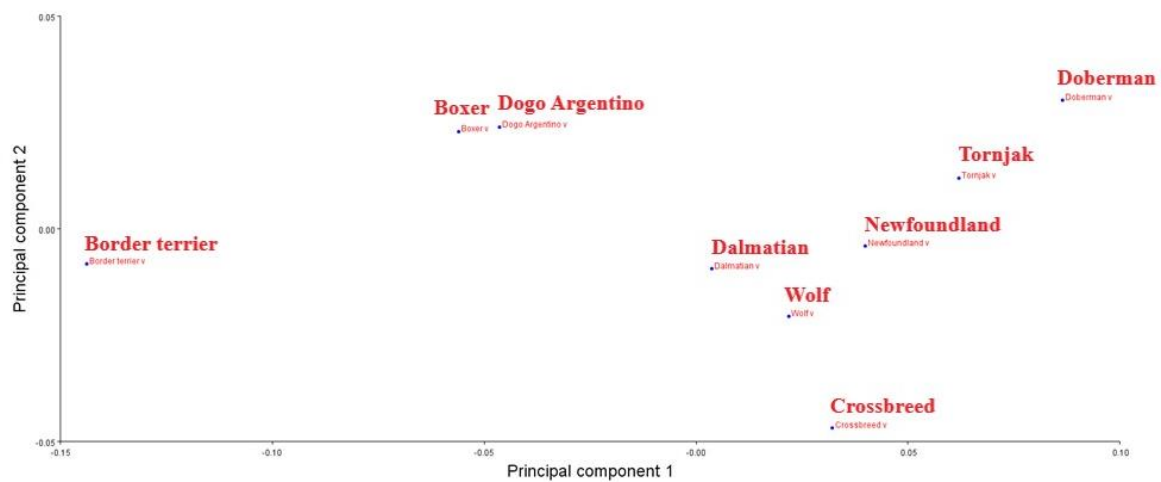


Figure 24. Graphical representation of the results from comparing Principle Component 1 vs Principle Component 2 of the ventral aspect landmarks.

Figure 25 is a wireframe graph of the lateral ventral landmarks from the skull of the Border terrier dog breed superimposed with the mean ventral aspect landmarks from all the skulls used in the Procrustes analysis

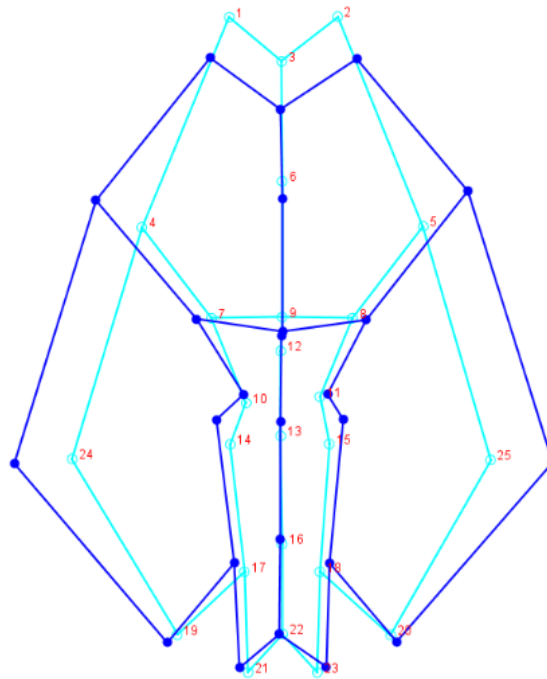


Figure 25. Wireframe comparison of ventral landmarks from the Border terrier dog breed (dark blue) and the mean landmarks (light blue).

Figure 26 is a wireframe graph of the ventral aspect landmarks from the skull of the Boxer dog breed superimposed with the mean ventral aspect landmarks from all the skulls used in the Procrustes analysis.

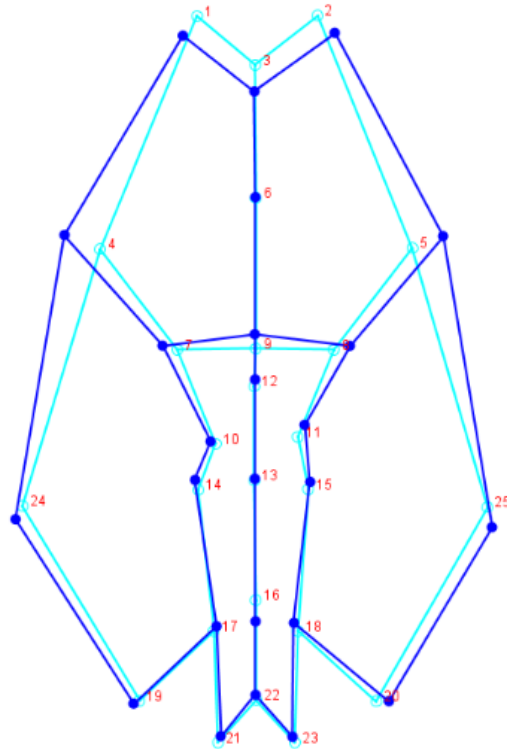


Figure 26. Wireframe comparison of ventral landmarks from the Boxer dog breed (dark blue) and the mean landmarks (light blue).

Figure 28 is a wireframe graph of the ventral aspect landmarks from the skull of the Dalmatian dog breed superimposed with the mean ventral aspect landmarks from all the skulls used in the Procrustes analysis.

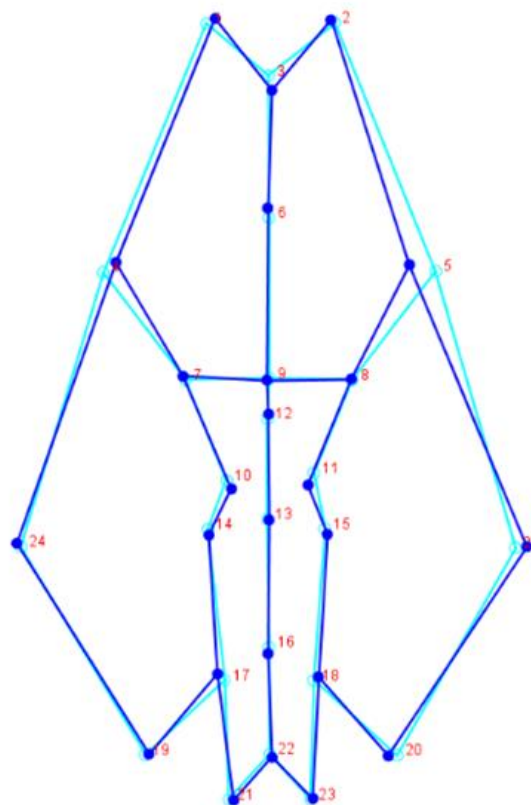


Figure 27. Wireframe comparison of ventral landmarks from the Dalmatian dog breed (dark blue) and the mean ventral landmarks (light blue).

5. DISCUSSION

The aim of this study was to take measurements from a variety of dog skulls in order to determine a method which would best identify the closest breed of unknown dog remains based on their skull morphology. The main methods used in this study were calliper-based morphometrics, digital image-based morphometrics, and geometric morphometrics (ADAMS et al., 2004)

Firstly, the calliper-based method is widely used and has historically been a relatively accurate, reliable, and inexpensive method, with minimal training needed for its use. The limitation of this is the human error associated with an analogue calliper, as well as the lack of accuracy up to two decimal points. It is also quite a time-consuming process and usually requires the analyst to take repeat measurements to decrease the percentage of error. Since the introduction of digital callipers, the accuracy of measurements has been significantly increased up to three decimal points and has eliminated the potential error made by the analyst when reading from the analogue calliper, however, it is still a laborious and limited process (MOTT et al., 2010). In this study both callipers were used, with the analogue calliper used only for the measurement M1 (Total length of skull) for each skull and the digital calliper used for the remaining measurements. This was due to the size of digital calliper making it unable to capture the total length of every skull. Although this means that M1 may not be as accurate as the other measurements, the calliper was used systematically for this single measurement and therefore, should not significantly affect the results when comparing the skull measurements of each breed.

The results from this study show that 8 out of 14 measurements were normally distributed (depicted in Table 11) and were used for further analysis. After performing one-way ANOVA tests, comparing those 8 measurements to each breed, there was significant statistical differences in 7 of the 8 measurements (excluding M7, Figure 8) for the breeds of which data was collected. The results of the ANOVA testing show few trends, with the Dalmatian, unspecified Terrier and unknown skulls (NA) having some of the lowest measurements, whereas the Dogo Argentino, Newfoundland and the Wolf have often the largest measurements, as well as many measurements being increased for the Border terrier.

The measurements taken from the digital images of the representative skulls showed differences when compared to the calliper measurements. A comparative statistical test of the two sets of measurements was considered, however, it would be difficult to attribute any

statistical significance to either one of the methods due to the fact that neither can be considered standardised measurements to compare to. In the study performed by MOTT et al. (2010), they state that "...digital image-based measurements were significantly more accurate, faster to obtain, and resulted in reduced inter-observer measurement variation relative to calliper measurements, yet the former was associated with reduced precision among repeated measurements relative to the latter."

The indices for the representative skulls were calculated from the digital image measurements and were based on the index formulas described EVANS and DE LAHUNTA (2013) and KOCH et al. (2012). Indices from this study were compared to the average indices for each classification of dog skull morphology (i.e., brachycephalic, mesocephalic, dolichocephalic) which was stated in the aforementioned literature and therefore, a conclusion can be made that the indices from our samples are similar to those in the literature and align with the classification of each dog skull.

A significant limitation to these morphometric methods is the large correlation of measurements and breed size (BOOKSTEIN et al., 1985). The large and giant dog breeds, as well as the wolf species, will naturally have larger skulls and thus can affect the results when attempting to compare them to smaller individuals of the same breed or smaller breeds of the same classification. Furthermore, as stated by ADAMS et al. (2004), it is not possible to produce graphical representations of the dog skulls using only linear distance measurements and therefore, many aspects of shape are lost. This can result in my measurements being unreliable when deciding to classify or identify a dog skull of unknown breed. These limitations to traditional linear morphometry allow for the introduction of geometric morphometrics.

Geometric methods have been used more frequently in the last couple of decades as higher imaging techniques have become more readily accessible ADAMS et al (2004). The majority of studies using geometric morphometrics on dog skulls have used Computed Tomography and/or the Microscribe digitiser. The goal of these methods is to use landmark and outline techniques to compare only the shape element of skulls, by removing data related to size, position, and rotation. (DRAKE et al., 2017)

In this study, digital images were taken of dorsal, ventral, and lateral aspects of each representative skull and landmarks were chosen based on the scientific paper by DRAKE et al. (2010), as well as some additional landmarks based on their anatomical locations. The lateral aspect landmarks in this study were chosen based on their anatomical significance and expected

variability within the breeds. By using the tpsDig2 program, static and curved landmarks were created for each skull aspect and imported into MorphoJ software (KLINGENBERG, 2011) which performed a Procrustes superimposition of every landmark coordinate (Figure 9). This superimposition graphically represents the means of every landmark as the bold and numbered points, surrounded by the individual measured landmarks as smaller unnumbered points. Furthermore, a wireframe was created based on the mean landmarks to improve the visual representation of each aspect. A covariance matrix was generated in order to perform a Principal Component Analysis (PCA) for each of the three aspects of the dog breeds, represented by Figures 10, 14, and 18. These PCAs allow for the visualisation of variance amongst our sample of breeds. In the PCAs, the breeds which cluster together share similar characteristics and the breeds that are furthest from those will show higher variance according to either PC1 or PC2. For the dorsal landmarks, the Border terrier breed shows the most variance for PC1, with the Tornjak and Doberman variance influenced more by PC2. The rest of the breeds cluster and therefore, it would be difficult to distinguish them individually. In the PCA of the ventral landmarks, the Doberman breed shows the greatest variance according to PC1, the Border terrier according to PC2, while the Boxer and Dogo Argentino form one cluster and the remaining breeds also cluster relatively close together. This is interpreted as the Doberman showing the most variance on the ventral aspect, the Boxer showing the second most variance, but according to the measurements that influence PC2, and the remaining breeds showing similar variance. Lastly, the PCA for the lateral aspect shows the most variance for the Doberman and Dalmatian for the measurements that influence PC1 and the most variance for the measurements that influence PC2 is attributed to the Border terrier. The Boxer and Dogo Argentino breeds form a cluster while the rest of the breeds are relatively clustered together also.

Limitations with the geometric morphometric methods are variable. Firstly, they are dependent on our sample size, variety of dog breeds, as well as the competence of the analyst. It should be noted that these methods are significantly more complex than the calliper-based or digital-image base morphometrics. In addition, no further statistical tests were able to be conducted on the PCA matrices generated due to the limited sample size. Furthermore, the variety of breeds in this study was limited and thus an accurate representation of the total variance of the dog skull could not be incorporated. Lastly, in this study, digital photographic imaging was used which limits the potential accuracy and types of analyses that could be performed when compared to using e.g., Computed Tomography, such as in DRAKE et al. (2017). However,

there were methods for reducing the errors in this study by ensuring consistency in the technology (digital camera and software), the photographic background such as, lighting and distance from the camera, and lastly, ensuring that the skulls are stabilised.

With regards to the field of archaeozoology, the methods used in this study can be useful to compare the unknown skulls found in archaeological excavations, to those of known breeds. TRBOJEVIĆ VUKIČEVIĆ et al. (2009) used the mesocephalic breed of the Dalmatian dog as a comparative tool using traditional calliper-based morphometrics. A similar approach could be given to geometric morphometrics, by comparing a skull of a known breed to the archaeozoological specimen, or by comparing the skull of unknown breed to the mean from the sample of known breed skulls and drawing conclusions from their similarities and/or differences.

6. CONCLUSIONS

1. Traditional morphometrics (calliper-based and/or image-based) still have a prominent role in craniometry and are necessary for further analyses.
2. Geometric morphometrics have a significant role in the analysis of skull shape and can provide information that traditional morphometrics cannot.
3. Both the traditional and the geometric morphometric methods are unable to firmly identify specific breeds in this study.
4. Certain breeds showed similarities with each other in both traditional and geometric morphometrics.
5. The sample size of the study and the lack of variety of dog breeds may have been the main factors for the lack of ability to identify breeds.
6. A similar approach could be given to comparing a skull of a known breed to the archaeozoological specimen by comparing the skull of unknown breed to the mean from the sample of known breed skulls and drawing conclusions from their similarities or differences.

7. REFERENCES

- ADAMS, D. C., F. J. ROHLF, D. E. SLICE (2004): Geometric morphometrics: Ten years of progress following the ‘revolution.’ *Ital. J. Zool.*, 71, 5–16. doi.org/10.1080/11250000409356545
- ANDREIS, M. E., U. POLITO, M. C. VERONESI, M. FAUSTINI, M. DI. GIANCAMILLO, S. C. MODINA (2018): Novel contributions in canine craniometry: Anatomic and radiographic measurements in newborn puppies. *PLoS ONE*, 13(5), 1–13. doi.org/10.1371/journal.pone.0196959
- BARDUA, C., R. N. FELICE, A. WATANABE, A-C. FABRE, A. GOSWAMI (2019): A Practical Guide to Sliding and Surface Semilandmarks in Morphometric Analyses. *Integr. Comp. Biol.* 1, 1-34. doi.org/10.1093/iob/obz016
- DRAKE, A. G., M. COQUERELLE, P. A. KOSINTSEV, O. P. BACHURA, M. SABLIN, A. V. GUSEV, L. S. FLEMING, R. J. LOSEY (2017): Three-Dimensional Geometric Morphometric Analysis of Fossil Canid Mandibles and Skulls. *Sci. Rep.*, 7, 1–8. doi.org/10.1038/s41598-017-10232-1
- DRAKE, A., G., C. P. KLINGENBERG (2010): Large-scale diversification of skull shape in domestic dogs: Disparity and modularity. *Am. Nat.*, 175, 289–301. doi.org/10.1086/650372
- DRAKE, A., G., M. COQUERELLE, G. COLOMBEAU (2015): 3D morphometric analysis of fossil canid skulls contradicts the suggested domestication of dogs during the late Paleolithic. *Sci. Rep.*, 5, 1-8.
- JEDRZEJOWSKA, Z. K. (2001): Craniometry and mathematical calculations as a method for viscerocranium profile determination. *Forensic Sci. Int.* 117, 145–151. doi.org/10.1016/S0379-0738(00)00456-4
- KLINGENBERG, C. P. (2011). MorphoJ: An integrated software package for geometric morphometrics. *Mol Ecol Resour.* 11, 353–357. doi.org/10.1111/j.1755-0998.2010.02924.x

- KOCH, D. A., T. WIESTNER, A. BALLI, P. M. MONTAVON, E. MICHEL, G. SCHARF, S. ARNOLD (2012): Proposal for a new radiological index to determine skull conformation in the dog. *Schweiz. Arch. Tierheilkd.*, 154, 217–220. doi.org/10.1024/0036-7281/a000331
- KOKOTSAKI, D., V. MENZIES, A. WIGGINS (2014): Durham Research Online Woodlands. *Crit Stud Secur*, 2, 210–222.
- LELE, S. (1993): Euclidean Distance Matrix Analysis (EDMA): Estimation of mean form and mean form difference. *Math. Geol.*, 25, 573–602. doi.org/10.1007/BF00890247
- MACLEOD, N. (2013): Landmarks and semilandmarks: differences without meaning and meaning without difference. *Palaeontological Association Newsletter*, 2013, 32–43.
- MAHDY, M. A. A., W. F. MOHAMED (2022): Comparative craniometric measurements of two Canid species in Egypt: the Egyptian red fox and the Egyptian Baladi dog. *BMC Vet. Res.*, 18, 1–13. doi.org/10.1186/s12917-022-03275-8
- MARCUS, L. F. (1990): Traditional morphometrics. In *Proceedings of the Michigan morphometrics workshop* (Vol. 2, pp. 77-122). Ann Arbor, USA: The University of Michigan Museum of Zoology.
- MOORE, M. K. (2013): Sex Estimation and Assessment. In: *Research Methods in Human Skeletal Biology* (Issue Chapter 11). Elsevier Inc. doi.org/10.1016/B978-0-12-385189-5.00004-2
- MOTT, C. L., S. E. ALBERT, M. A. STEFFEN, J. M. UZZARDO (2010): Assessment of digital image analyses for use in wildlife research. *Wildlife Biol*, 16, 93–100. doi.org/10.2981/09-010
- REITZ, E. J., E. S. WING (1999): *Zooarchaeology*. Cambridge University Press, Cambridge.
- REYMENT, R. A., J. F. ARANKI (1991): On the Tertiary genus *Soudanella* Apostolescu (1961) (Ostracoda, Crustacea). *J Micropalaeontol*, 10, 23-28.
- ROHLF, F. J., L.F. MARCUS (1993): A revolution morphometrics. *Trends Ecol. Evol.* 8, 129–132. doi.org/10.1016/0169-5347(93)90024-J

- ROHLF, F. J., R. E. BLACKITH, R. A. REYMENT (1972): Multivariate Morphometrics. *Syst. Biol.*, 21, 348–349. doi.org/10.1093/sysbio/21.3.348
- SCHOENEBECK, J. J., E. A. OSTRANDER (2013): The genetics of canine skull shape variation. *Genetics*, 193, 317–325. doi.org/10.1534/genetics.112.145284
- SLICE, D. E. (2007). Geometric morphometrics. *Annu. Rev. Anthropol.*, 36, 261–281. <https://doi.org/10.1146/annurev.anthro.34.081804.120613>
- TRBOJEVIĆ VUKIČEVIĆ, T., T. KOLAK, K. BABIĆ (2009): Dog or wolf? Implementation of veterinary osteology to archaeological case. Abstract book of 1st International Symposium of Clinical and Applied Anatomy (ISCAA),(Krivokuća, D., M. Erić , eds.). 17-19. rujna 2009. Novi Sad, Srbija. 167-167.
- VIGO, V., K. CORNEJO, L. NUNEZ, A. ABLA, R. RODRIGUEZ RUBIO (2020): Immersive Surgical Anatomy of the Craniometric Points. *Cureus*, 12(6). doi.org/10.7759/cureus.8643
- VON DEN DRIESCH, A. (1976): A guide to the measurement of animal bones from archaeological sites. Peabody Museum of Archaeology and Ethnology, Harvard University, Cambridge.
- WILEY, D. F., N. AMENTA, D. A. ALCANTARA, D. GHOSH, Y., J. KIL, E. DELSON, W. HARCOURT-SMITH, F. J. ROHLF, K. ST. JOHN, B. HAMANN (2006): Evolutionary Morphing. 431–438. doi.org/10.1109/visual.2005.1532826

8. SUMMARY

A craniometric analysis of dogs (*Canis familiaris*) for the purpose of identifying archeozoological material

Olivia Frances Kaloyianni

Craniometry has been used in multiple disciplines, including anthropology, forensic science, archaeozoology, and neuroscience. Multiple methods have been constructed for their use in craniometric studies. Traditional morphometrics, one-dimensional measurements are used from two set points, usually describing distance, such as length, width, or height, but also ratios and angles can be added. Geometric morphometrics, specifically landmark methods, two-dimensional (2D) or three-dimensional (3D) coordinates of morphological landmarks on the specimen are recorded in order to describe the shape of the specimen. This study aimed to use methods from both categories of morphometrics to compare 43 skulls, from 41 dogs and 2 wolves. Both calliper-based and digital image-based morphometrics yielded similar results, showing trends for larger breeds and the brachycephalic breeds in the samples. The geometric morphometric methods showed similar clusters of breeds showing similarities according to the Principal Component Analysis, as well as showing visible differences in certain breeds compared to the means of the sample. These approaches could be readily used for comparison and/or determination of archaeozoological specimens of dog skulls.

Key words: craniometry, dogs, calliper, digital morphometrics, geometric morphometrics

9. SAŽETAK

Kraniometrijska analiza pasa (*Canis familiaris*) u svrhu identifikacije arheozoološkog materijala

Olivia Frances Kaloyianni

Kraniometrija se koristi u više disciplina, uključujući antropologiju, forenziku, arheozoologiju i neuroznanost. Za upotrebu u kraniometrijskim studijama konstruirano je više metoda. Tradicionalna morfometrija, odnosno jednodimenzionalna mjerenja koriste dvije zadane točke koje obično opisuju udaljenosti, kao što su duljina, širina ili visina, ali se mogu dodati i omjeri i kutovi. Geometrijska morfometrija, točnije orijentirne metode, koriste dvodimenzionalne (2D) ili trodimenzionalne (3D) koordinate morfoloških orijentira na uzorku kako bi se opisao njegov oblik. Ovo istraživanje imalo je za cilj korištenje obje morfometrijske metoda za usporedbu 43 lubanje, od čega 41 lubanju psa i 2 vuka. Morfometrija temeljena na pomičnoj mjerki i na digitalnoj slici dala je slične rezultate, pokazujući trendove za veće i brahiocefalične pasmine. Geometrijske morfometrijske metode pokazale su slične skupine pasmina prema analizi glavne komponente, kao i vidljive razlike u pojedinim pasmina u odnosu na srednje vrijednosti uzorka. Navedeni pristupi mogu se koristiti za usporedbu i/ili određivanje arheozooloških uzoraka lubanja pasa.

Ključne riječi: kraniometrija, psi, morfometrija pomična mjerka,, digitalna morfometrija, geometrijska morfometrija

10. BIOGRAPHY

Olivia Frances Kaloyianni was born in Kerkyra (Corfu), Greece on the 13th of February 1997. She completed her high school education 4th General High School of Kerkyra and went on to complete a Foundation Year (Science) at the University of Nottingham in the United Kingdom during the academic year of 2015/2016. Since September 2016, she has embarked on a degree at the Faculty of Veterinary Medicine, University of Zagreb as one of the students of the first generation of Veterinary Medicine in English. Together with a few of her colleagues, she co-founded the students' association, the Vet Society, of which she was President from 2018-2020. During this time, the Vet Society led numerous projects, including the renovation of the student room at the Department for Anatomy, Histology and Embryology. She has worked as a student demonstrator for the Anatomy courses and has participated in research work with Professor Tajana Trbojević Vukičević which was presented at congresses in Hannover and Bucharest.